Geologia Croatica
Journal of the Croatian Geological Survey and the Croatian Geological Society
2026 | 79/1 | 45–67 | 21 Figs. | 6 Tabs. | www.geologia-croatica.hr

Paragenetic interpretation of Ti-clinohumite-bearing marble from Zorovac Creek, Mt. Moslavačka Gora (Croatia) and its petrogenesis

Vesnica Garašić[1] and Šime Bilić[1,*]

[1] University of Zagreb, Faculty of Mining, Geology and Petroleum Engineering, Pierottijeva 6, 10 000 Zagreb, Croatia;
(*corresponding author: sime.bilic@rgn.unizg.hr; vesnica.garasic@rgn.unizg.hr)

doi: 10.4154/gc.2026.05

Crossref Similarity Check

Article history:
Manuscript received: April 26, 2024
Revised manuscript accepted: December 1, 2025
Available online: February 25, 2026

Abstract

This study examines impure grey marble occurring as interlayers in amphibolite and diopside-amphibole schists which belong to the magmatic-metamorphic complex of Mt. Moslavačka Gora in Croatia. The marble is composed mainly of calcite with abundant accessory minerals: dolomite, forsterite, spinel, pargasite, phlogopite, ilmenite, apatite, Ti-clinohumite, tremolite, chlorite, serpentine and talc. Detailed descriptions of mineral assemblages, their textural relationships and mineral chemistry analyses *in situ,* as well as compositional maps of characteristic mineral assemblages, revealed that the marble experienced at least three different metamorphic stages. These can be summarized as follows: a) the regional metamorphic stage characterised by peak metamorphic stage in granulite facies and a mineral assemblage consisting of calcite + dolomite + forsterite + spinel + pargasite + phlogopite + ilmenite + apatite; b) the stage of subsequent infiltration of an external Ti-rich, fluorinated fluid into the marble giving rise to the origin of Ti-clinohumite, the Ti content of which varies from 0.070 to 0.325 pfu and its X_F value, defined as F/(F + OH), is in the range of 0.32 to 0.57; c) the stage of uplift and exhumation of the terrain causing diverse retrograde metamorphic reactions such as the replacement of Ti-clinohumite, spinel and pargasite by chlorite, formation of tremolite on the rims of pargasite and forsterite, as well as the replacement of forsterite by serpentine and talc. Due to the differences in the age determinations of both metamorphisms and magmatic intrusions, good correlation between the occurrence of the Ti-clinohumite bearing marbles of Mt. Moslavačka Gora with those found in surrounding terrains, for instance in Alps (Switzerland/Italy, Austria, Czech Republic) and Rhodope massif (Greece), could not be established at this stage of the investigation.

Keywords: Ti-clinohumite, Ti-rich fluorinated fluid, granulite-facies marble, polyphase metamorphism, Mt. Moslavačka Gora

1. INTRODUCTION

The occurrence of uncommon minerals in marbles may reflect the composition of protoliths or point to the infiltration of externally derived fluids promoting metamorphic reactions at any point in the marble's history.

One such uncommon mineral in marbles is certainly clinohumite, a rare hydrous magnesium iron silicate, belonging to the humite group, with a general formula $nM_2SiO_4{*}M_{1-X}Ti_X(OH,F)_{2-2X}O_{2X}$. M stands for octahedrally coordinated Mg, Fe, Mn, Ca and Zn cations in descending order of abundance, x<1 and n = 1, 2, 3, 4 for norbergite, chondrodite, humite and clinohumite (JONES et al., 1969). The appearance of clinohumite in nature is restricted only to six rock types: kimberlites (MCGETCHIN et al., 1970), Archean ultramafics (NISHIO et al., 2019), Alpine peridotites (TROMMSDORFF & EVANS, 1980; EVANS & TROMMSDORFF, 1983; MENZEL et al., 2019), carbonatites (GASPAR, 1992), skarns (RIOS et al., 2015) and marbles (RICE, 1980; HIROI & KOJIMA, 1988; KARMAKAR, 2021; CHEN et al., 2022; BOUREGHDA et al., 2023).

Increasing attention has been given recently to clinohumite not only because of its importance in the understanding of volatile recycling and geodynamic processes in the Earth's mantle (SÁNCHEZ-VIZCAÍNO et al., 2005; HUGHES & PAWLEY, 2019), but also in deciphering Ti mobility in the framework of crustal metamorphism associated with clinohumite formation in forsterite marbles (KARMAKAR, 2021). Numerous studies have revealed that the humite minerals occurring in ultrabasic rocks are usually enriched in titanium and poor in fluorine, whereas those found in carbonate rocks are poor in titanium but rich in fluorine (e.g., RICE, 1980). An equilibration at high to ultrahigh pressure metamorphic conditions and high temperatures is usually proposed for Ti-rich clinohumites occurring in ultramafic rocks, as described for example for Ti-rich clinohumite in the peridotites of the Cabo Ortegal complex in Spain (GIL IBARGUCHI et al., 1999). The occurrence of humite minerals in marbles may be very important for correlation and interpretation of regional-scale orogenic events. For instance, it was newly recognized that many humite-bearing granulite facies marbles worldwide are related to the dispersed Gondwanan fragments suggesting an Neoproterozic "East Gondwana-wide humite-epoch" characterized by fluorinated, very rich aqueous fluid activity during the waning stages of the Pan-African orogeny (PRADEEPKUMAR & KRISHNANATH, 2000; FERNANDES & CHAVES, 2014; PIAZOLO & MARKL, 1999).

The only documented clinohumite occurrence found in Croatia up to this time is in the grey marbles of Zorovac Creek in Mt. Moslavačka Gora (BARIĆ, 1972; GARAŠIĆ, 1993; BALEN et al., 2000). These marbles represent a part of the magmatic-metamorphic complex of Mt. Moslavačka Gora, which comprises high- to medium-grade metamorphic rocks intruded by different types of granitoid rocks.

This study aims to characterize different metamorphic stages in the evolution of Ti-clinohumite-bearing impure marble from Zorovac Creek, using detailed descriptions of mineral assemblages, their textural relationships and mineral chemistry analyses *in situ*, as well as compositional mapping of samples. Such detailed study has never been done before on these marbles. The recognition of different metamorphic stages in the marble history based on careful examination of mineral assemblages could provide additional constraints on the partially resolved evolution of the magmatic-metamorphic complex of Mt. Moslavačka Gora in Croatia.

2. GEOLOGICAL SETTING

The studied Ti-clinohumite is found in grey marbles appearing as interlayers up to 50 cm thick, in amphibolite and diopside-amphibole schists. All these rocks belong to the magmatic-metamorphic complex of Mt. Moslavačka Gora. This crystalline complex occurs as an inselberg, covering an area of about 180 km^2, in the southwestern part of the Pannonian Basin characterised by Neogene and Quaternary sedimentary infill (PAMIĆ, 1990). Previously, this crystalline complex in the context of plate tectonics, was regarded as being a part of the Tisza mega unit (PAMIĆ, 1998; PAMIĆ & JURKOVIĆ, 2002). However, in recent studies it is attributed to the Sava zone (SCHMID et al., 2008; USTASZEWSKI et al., 2008; STARIJAŠ et al., 2010; BALEN & PETRINEC, 2011), due to the recognized dominant Cretaceous igneous and metamorphic imprint. According to SCHMID et al. (2008) the Sava zone represents the suture between Europe and the Adria-derived tectonic units in the area between the Pannonian Basin and the Dinarides (Fig. 1).

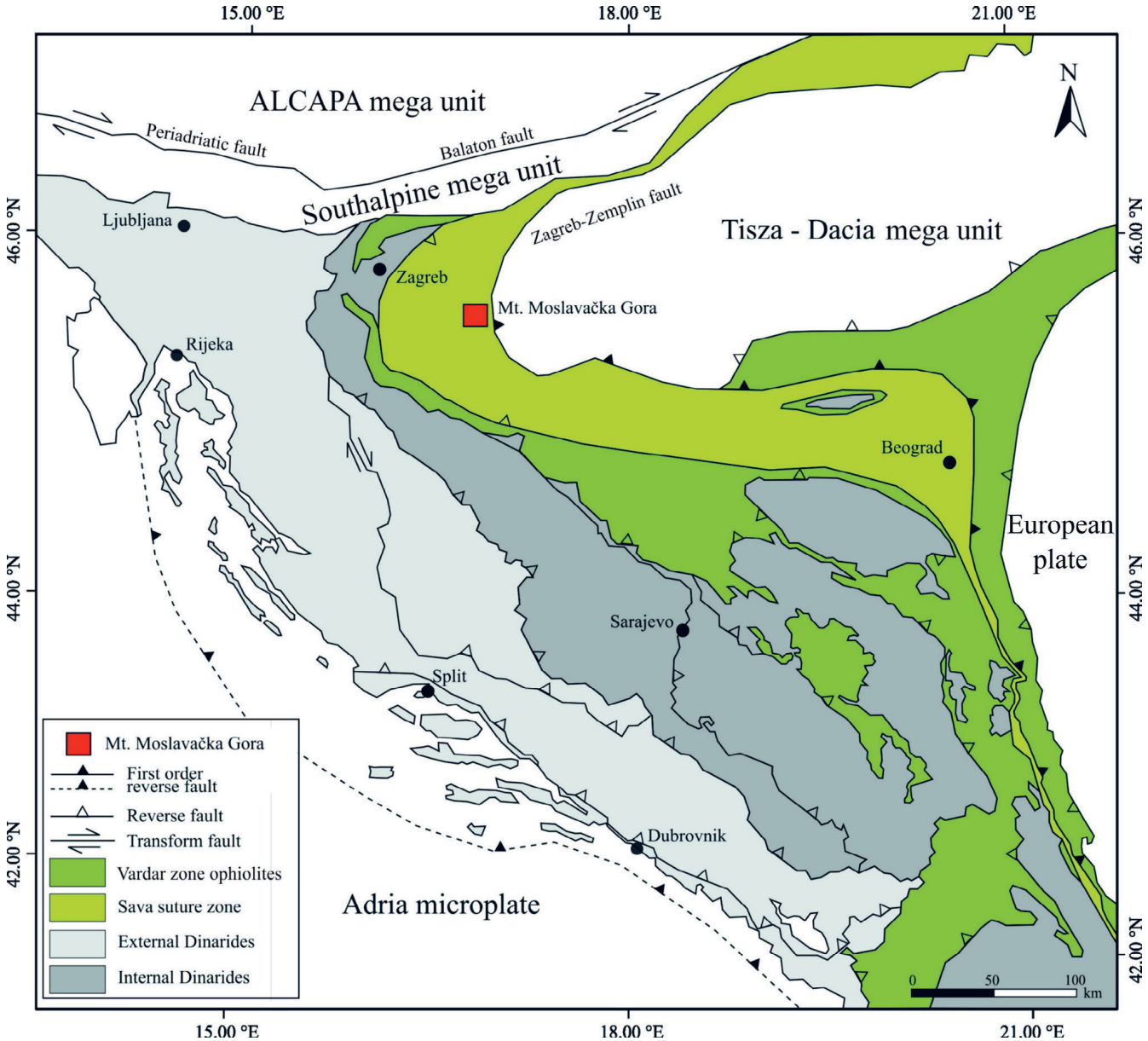

Figure 1. The position of Mt. Moslavačka Gora within the major regional tectonic context (based on SCHMID et al., 2008) and modified after GARAŠIĆ et al. (2024).

As described in an overview recently published by GARAŠIĆ et al. (2024), the magmatic-metamorphic complex of Mt. Moslavačka Gora (Fig. 2) comprises high- to medium-grade (mainly migmatite, orthogneiss and paragneiss) and medium-grade metamorphic rocks (mostly micaschist and amphibolite), with rare intercalations of quartzite and marble (TUĆAN, 1953; BARIĆ, 1972; CRNKO & VRAGOVIĆ, 1990; GARAŠIĆ, 1993; BALEN et al., 2000). This metamorphic rock sequence was intruded by different granitoid rocks (two-mica granite, granodiorite, monzogranite and leucogranite), as reported by CRNKO & VRAGOVIĆ (1990) and PAMIĆ (1990), as well as by different types of gabbro (KIŠPATIĆ, 1887; TUĆAN, 1953; PAMIĆ, 1987; BALEN et al., 2003) and monzodiorites (PAMIĆ, 1987). The granitoid intrusions caused the fragmentation of an older metamorphic complex and CRNKO & VRAGOVIĆ (1990) regarded parts of these metamorphic rocks as blocks and xenoliths. Although in the immediate vicinity of Zorovac Creek the abandoned quarry of granite and monzodiorite and gabbro (PAMIĆ, 1987) exists (Kamenac Creek), no contacts between marble and magmatic rocks were observed. Due to the very rare outcrops of marbles, which are then additionally covered by soil and vegetation, it is impossible to deduce clear relationships between marbles and all amphibole-bearing metamorphic rocks and metapelites occurring in the area.

It should be emphasized that andalusite, sillimanite and tourmaline were found in some of the granitoid bodies (COHEN, 1887; KIŠPATIĆ, 1887; CRNKO & VRAGOVIĆ, 1990; GARAŠIĆ et al., 2007; BALEN, 2007; BALEN & PETRINEC, 2010; BALEN & BROSKA, 2011), suggesting S-type granitic magmas. Pegmatite and aplite dykes occur mainly in migmatite and granitic rocks (TUĆAN, 1904; CRNKO &

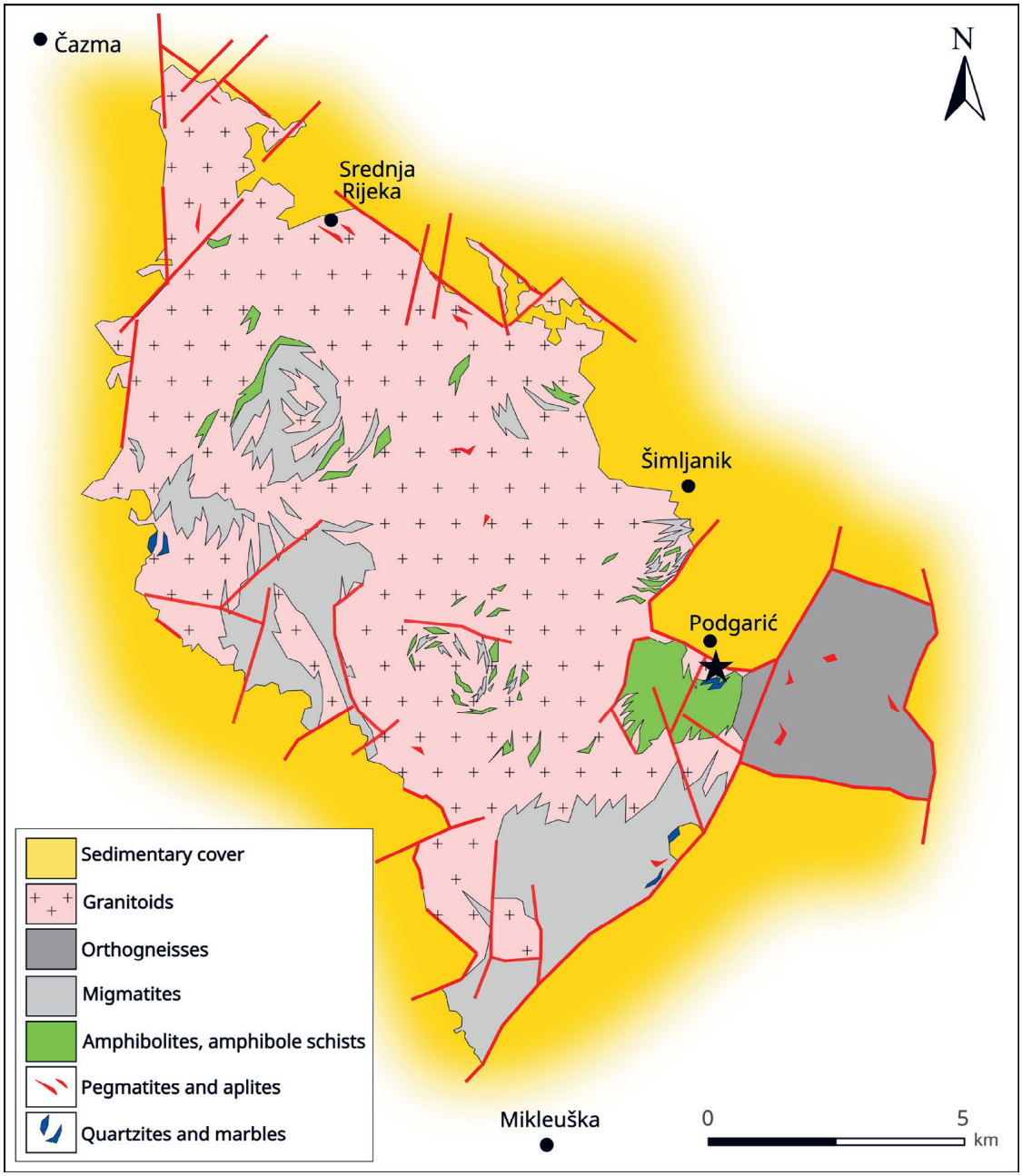

Figure 2. Geological sketch map of Mt. Moslavačka Gora (based on CRNKO, 1990 and KOROLIJA & CRNKO, 1985), with sample locations marked by a black star. Modified after GARAŠIĆ et al. (2024).

VRAGOVIĆ, 1990). Study of rare dumortierite-bearing pegmatite revealed that it is quite unique when compared with other dumortierite-bearing pegmatites worldwide since it originated by fraction crystallisation from a granitic melt (GARAŠIĆ et al., 2024). It is also important to highlight that the primary blue dumortierite was replaced by secondary purple dumortierite due to the later circulation of Ti-rich hydrothermal fluids (GARAŠIĆ et al., 2024). The appearance of contrasting types of enclaves in granites described by BALEN & PETRINEC (2010) points to a complex evolution for some of the granitic rock types found in Mt. Moslavačka Gora. PETRINEC & BALEN (2014) determined a Cretaceous S-type granitoid metamorphic event reaching ≈ 8 kbar and max. ≈ 800 °C in amphibole-bearing xenoliths and a later LP-HT event (100 – 90 Ma), characterised with 2 – 5 kbar and ≈ 720 – 790 °C in metapelitic rocks. According to these authors, both events preceded the Late Cretaceous intrusion of the central granitoid body. More recently, PETRINEC & BALEN (2019) investigated cordierite-bearing metapelitic rocks from different localities of Mt. Moslavačka Gora and found that they all are anatexites, characterized by different degree of melt generation and segregation. The authors described prograde and retrograde cordierite production reactions and the occurrence of cotectic magmatic cordierite. Additionally, closer investigation of macro- and microscale textural uniformity of amphibolite xenoliths in two-mica granite of Mt. Moslavačka Gora, revealed that the melt production reaction (Hbl + Pl ± Qtz ± Ilm = Di ± Ttn ± Grt ± Opx + melt), occurred before incorporation of the xenolith into the intruding granite magma (PETRINEC et al., 2022). These authors emphasized that this is not in accordance with the prevailing older interpretation which claims that an S-type granite pluton caused the migmatisation of the metamorphic rocks of Mt. Moslavačka Gora.

Available geochronological data indicate a long period of geological evolution for the Mt. Moslavačka Gora magmatic-metamorphic complex. An Early Ordovician age (486 – 491 Ma) was obtained by dating of magmatic zircon cores in orthogneisses which were interpreted as representing the remnants of Ordovician granitic crust, related to the rifting of the northern Gondwana margin (STARIJAŠ et al., 2010). The Late Cretaceous age (90 – 100 Ma) is documented by monazite dating in metapelites and is explained as the granulite facies LP/HT metamorphic overprint at 750 ºC and 3 – 4 kbar (STARIJAŠ et al., 2010). Similar values (80 – 90 Ma) are gained from Ar-Ar amphibole dating in amphibolites (BALEN et al., 2001). In addition, a magmatic zircon age determined from the Central granite, which intruded the metamorphic rocks, corresponds to 82 ± 1 Ma (STARIJAŠ et al., 2010), and agrees with the Ar-

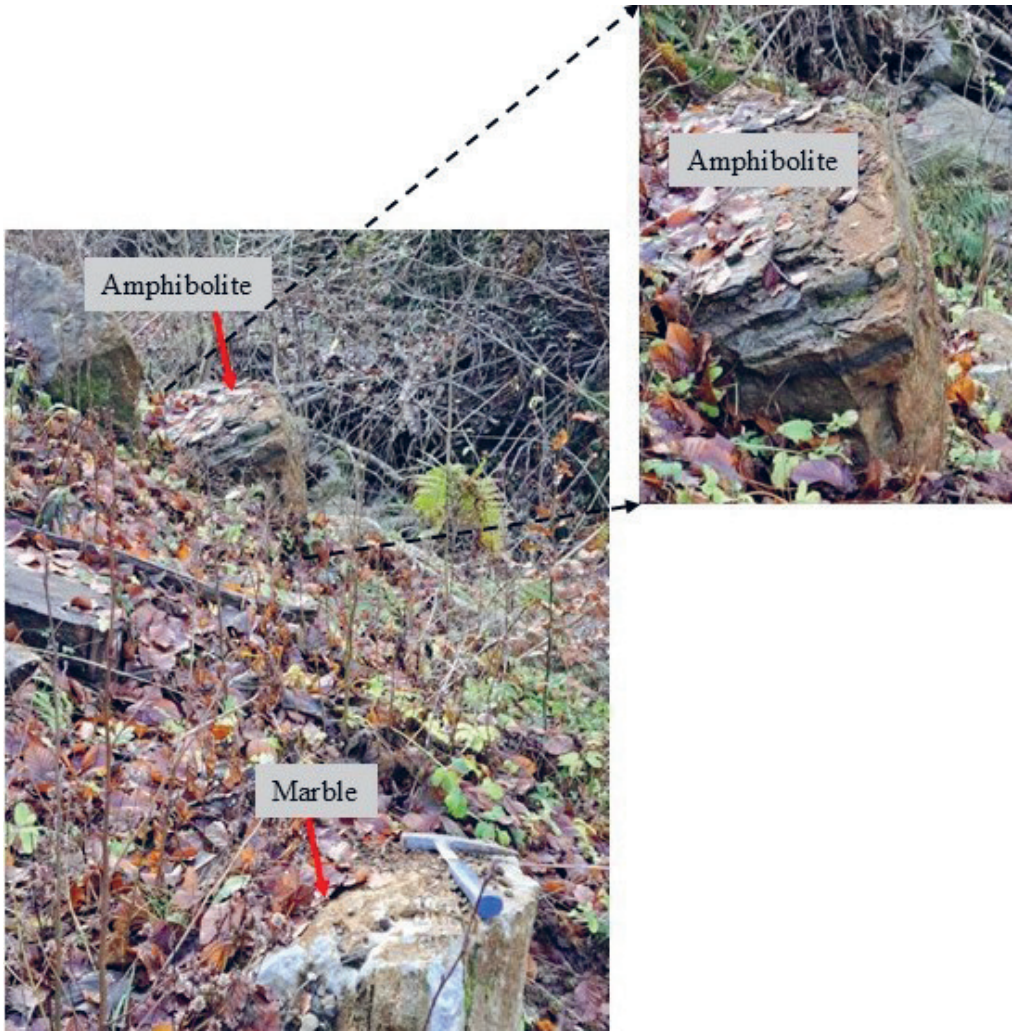

Figure 3. Field relationships on the bank of the Zorovac Creek between marble and amphibolite / diopside-amphibole schists.

Ar muscovite cooling ages of 73 ± 1 and 74 ± 1 Ma for pegmatite dykes fractionated from the Central granite (PALINKAŠ et al., 2000; BALEN et al., 2001). Additionally, clinopyroxene, plagioclase and whole rock isotopic data from an olivine gabbro, related to the upper mantle melt, yielded a Sm-Nd isochrone age of 109 ± 8 Ma (BALEN et al., 2003).

3. ANALYTICAL METHODS

3.1. Fieldwork

The marble samples were collected from one of the very rare outcrops on the bank of the Zorovac Creek (GPS coordinates: 45º63'38'' N/ 16º78'26'' E). The Zorovac Creek is located approximately 1 km south of the settlement of Podgarić in the eastern part of Mt. Moslavačka Gora (Fig. 2). Marbles occur as interlayers up to 50 cm thick in amphibolite and diopside-amphibole schists (Fig. 3). A large part of the studied outcrop is covered by vegetation with developed soil in places and therefore it is not possible to define the primary relationships between the marbles and amphibolite and diopside-amphibole schists.

3.2. Optical microscopy

Five marble samples (MG8, MG9, MG10, MG11, and MG12) were chosen, based on differences in their colour and grain size, for microscopic investigations. The petrographic characteristics and mineral assemblages in the marbles were determined using standard 30-µm thin sections of rock samples under polarised light microscope (a Leica Microsystem 020-522 101 DM/LSP with 4x, 10x and 40x magnifications), at the University of Zagreb Faculty of Mining, Geology and Petroleum Engineering, Department of Mineralogy, Petrology and Mineral Resources. Photomicrographs were taken by the CCD (1"; SONY EXVIEW) camera associated with an Optika B1000 Pol-I polarizing microscope and Proview software in the same Department.

3.3. Electron microprobe

Two marble samples (MG10 and MG11) were selected for study of their mineral chemistry, due to the presence of the most diverse mineral assemblages. Analysis was undertaken using the Cameca SX50 electron microprobe, at the Institute for petrography and geochemistry of the Fridericiana University of Karlsruhe (Germany), equipped with four wavelength-dispersive crystal spectrometers. The measurement conditions were an accelerating voltage of 15 kV, beam current of 10 nA, about 1 µm beam diameter and 20 s counting time for all elements except fluorine (40 s). Natural and synthetic silicates and oxides were used as calibration standards. The Cameca PAP matrix correction program was applied to convert raw data to wt.%. The computer program "Formelcalc" developed by Dr. Hans-Peter MEYER from the Institute of Geosciences, University of Heidelberg, Germany was used for mineral formula calculations. Besides *in situ* mineral analyses, compositional mapping was carried out using WDS spectra on representative parts of thin sections.

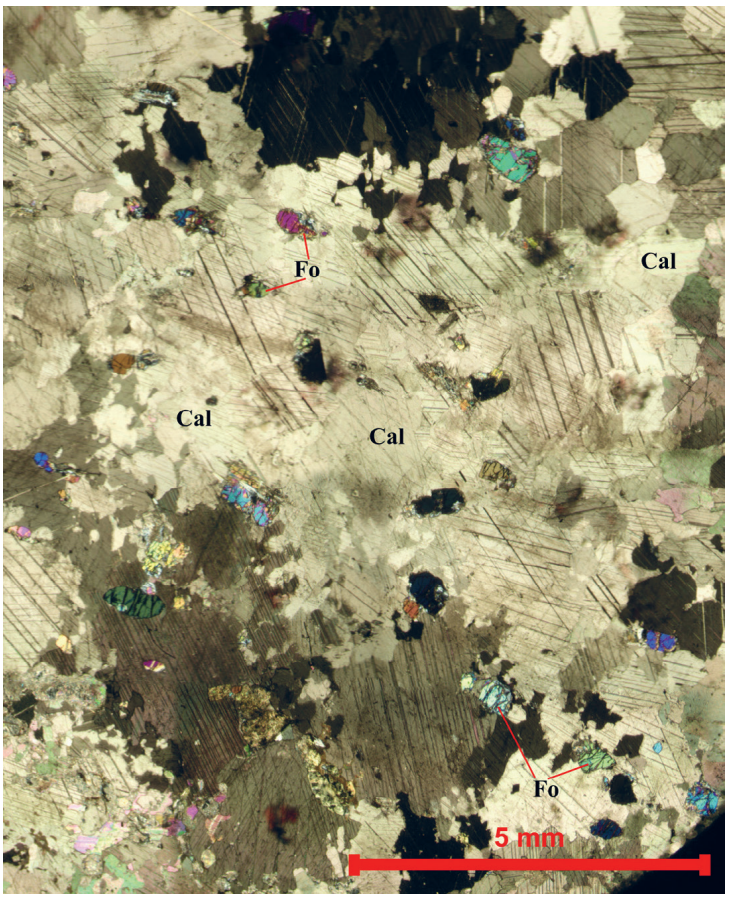

Figure 4. Granoblastic microstructure of grey marbles showing coarse calcite grains (up to 5 mm), and noticeably smaller silicate grains (up to 1 mm). The dominant silicate is forsterite, occurring mostly in tiny bands.

4. RESULTS

4.1. Petrography of grey marble

Macroscopically, it is possible to distinguish between grey (MG10, MG11), white-grey (MG8, MG12) and white (MG9) calcite marbles on the basis of mineral assemblages and grain size. Grey marbles are fine grained with an average grain size of about 1 to 2 mm, whereas white-grey and white marbles are characterised by coarser grains (approximately 4 mm). The grey marbles are composed mainly of calcite with abundant accessory minerals: dolomite, forsterite, serpentine, talc, amphibole, clinohumite, spinel, ilmenite, chlorite, phlogopite and apatite. White-grey marbles comprise almost the same minerals, excluding clinohumite and spinel. White marble has the same composition as the white-grey marble, but with the additional rare occurrence of diopside. This study concentrated on the grey marbles containing the most diverse mineral assemblages. Until now 24 minerals in different varieties of marble of Zorovac Creek have been recognized (BALEN et al., 2000), but clinohumite is very rare and was only found in the studied grey marble.

The microstructure of grey marbles is generally granoblastic. The distribution of accessory silicate minerals in marbles is not homogeneous (Fig. 4). They occur as tiny bands (≈ 5 mm) within which phyllosilicate minerals show partly preferred orientation. Silicates can also be found outside of these bands, forming clusters in the carbonate matrix. The grey marbles comprise 95.20 vol.% of carbonates (mainly calcite and only up to 2 vol.% dolomite) and 4.80 vol.% of silicate minerals, with dominant forsterite (3.5 vol.%), pargasite (0,5 vol.%), clinohumite (0.3 vol.%) and all other silicates (0.5 vol.%).

Calcite appears in the form of strain-free fine-grained grains, slightly variable in size (0.5 – 2 mm), and greatly exceeds dolomite by volume (Fig. 4, 5a).

Dolomite occurs as small exsolution patches in calcite, partly along calcite rims too, but mostly as anhedral grains at the rims of silicate minerals, especially forsterite (Fig. 5a, b).

Forsterite is the most frequent silicate mineral in the studied marbles. It forms subhedral to euhedral crystals (Figs. 5a, b, 6) up to 1 mm diameter or small anhedral grains having rounded forms (Fig. 7).

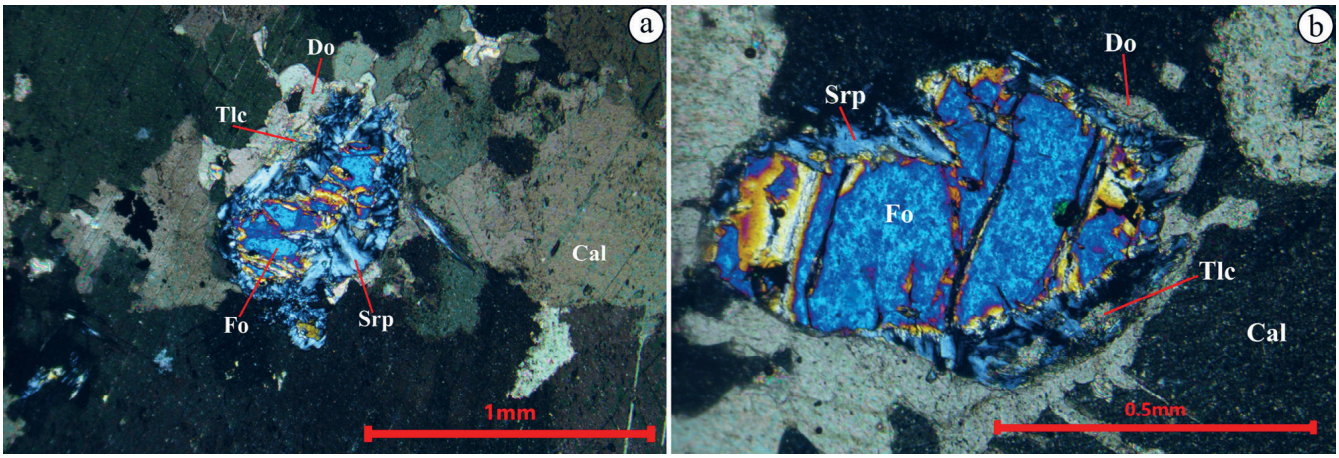

Figure 5. Photomicrographs of the Zorovac Creek impure calcite marble: **a** replacement of forsterite (Fo) in strain-free calcite (Cal) marble by serpentine (Srp), talc (Tlc) and dolomite (Do); **b** replacement of euhedral forsterite (Fo) crystals by narrow rim of dolomite (Do), serpentine (Srp) and talc (Tlc) in calcite (Cal) marble. The mineral abbreviations used in all figures are those recommended by WHITNEY & EVANS (2010).

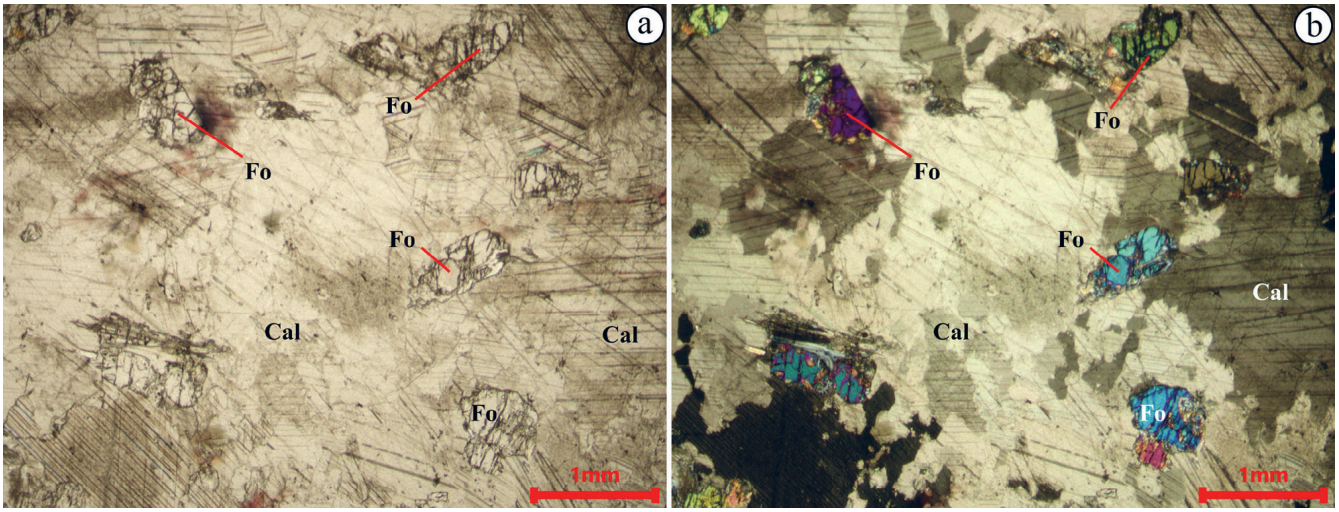

Figure 6. Photomicrographs of the euhedral crystals of forsterite (Fo) occurring with coarser calcite crystals (Cal): **a** under parallel nicols (N); **b** under crossed nicols (N+).

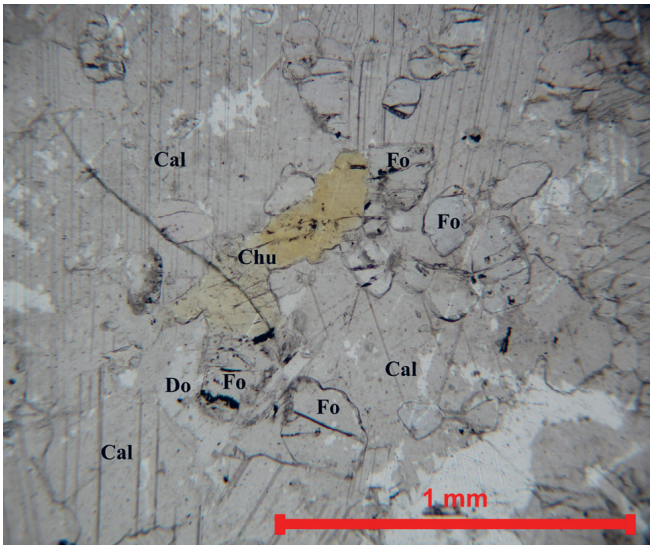

Figure 7. Photomicrographs of colourless small, rounded grains of forsterite (Fo) being partly replaced by yellow anhedral clinohumite (Chu) grains and dolomite (Do) in calcite (Cal) marble.

Serpentine generally appears as veins along olivine cracks and grain boundaries (Fig. 5a, b). Its pseudomorphs after olivine are only scarcely observed.

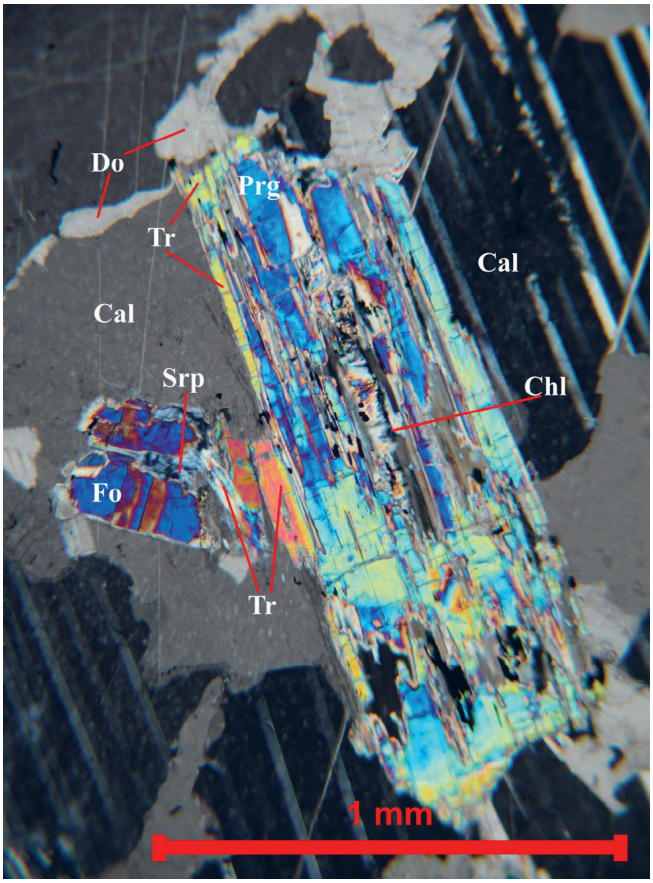

Figure 8. Photomicrographs of coarse euhedral prismatic grain of pargasite (Prg) showing readjustment of its composition to the prevailing PT conditions from pargasite core to the tremolite (Tr) rim and replacement by chlorite (Chl) along cracks in calcite (Cal) marble. Retrograde reaction between forsterite (Fo) and calcite (Cal) resulting in the development of tremolite (Tr) and dolomite (Do). The partial replacement of forsterite (Fo) by serpentine (Srp) is visible too.

Talc is usually present at the contact between olivine and calcite (Fig. 5a, b) or it completely replaces forsterite.

Clinohumite occurs abundantly as anhedral grains of different sizes replacing olivine. Macroscopically it is easy to identify due to its typical orange colour. In thin section, clinohumite displays a colourless to pale yellow and yellow pleochroism (Fig. 7).

Amphibole is observed as coarse euhedral prismatic grains (pargasite), being of about the same grain size as olivine or larger (1 – 2.5 mm) as shown in Figure 8, but also occurs as small prismatic crystals, or needle-like aggregates (tremolite), occurring at the rims of olivine (Fig. 9) and pargasite (Fig. 8).

Phlogopite is rare and occurs mostly in the form of individual flakes up to 0.25 mm in size (Fig. 10) occurring in a carbonate matrix. It displays a colourless to pale brown pleochroism and shows no reaction relationship to other

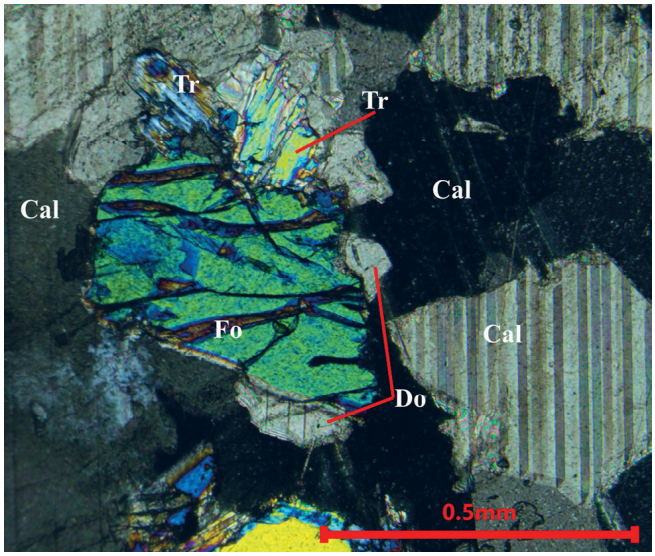

Figure 9. Photomicrographs of forsterite (Fo) with developed tremolite (Tr) and dolomite (Do) at its rims as a result of retrograde reactions between forsterite (Fo) and calcite (Cal).

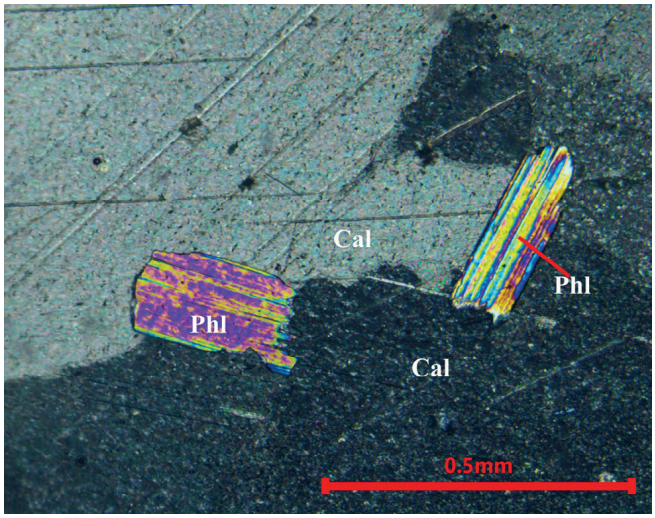

Figure 10. Photomicrographs of nicely developed individual phlogopite (Phl) flakes occurring in the calcite (Cal) matrix. No reaction relationship of phlogopite flakes to other mineral phases is visible.

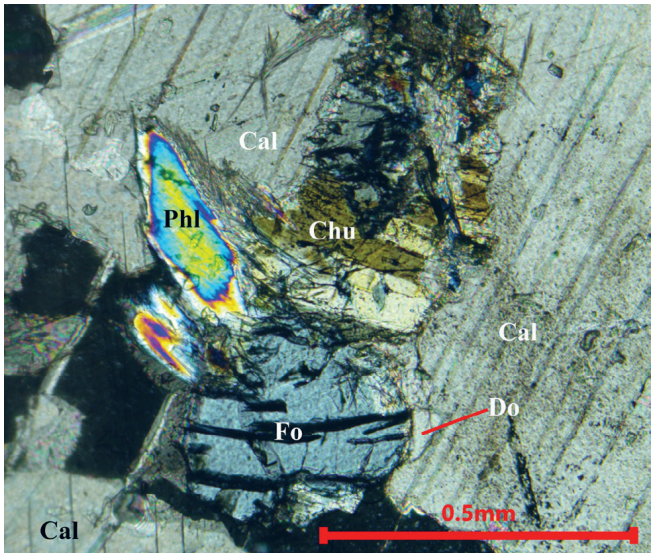

Figure 11. Photomicrographs of phlogopite (Phl), found only in this place, in reaction with other minerals as are forsterite (Fo), clinohumite (Chu), dolomite (Do) and calcite (Cal).

mineral phases. Phlogopite was found only in one place in a reaction relationship with other minerals (Fig. 11).

Spinel is colourless and forms small subhedral to euhedral grains up to 0.25 mm in diameter, occurring as isolated crystals in the calcite matrix or associated with silicates. It usually breaks down to coarse chlorite (Fig. 12a, b).

Opaque mineral, as a primary phase, is extremely rare, it was observed only as anhedral tiny grains included in pargasite or spinel, or in chlorite replacing pargasite or spinel.

Chlorite is represented by coarse flakes up to 1 mm in size. It is colourless, no pleochroism was observed. It replaces forsterite, clinohumite, spinel and pargasite (Fig. 12a, b).

Apatite is very scarce and appears as small, rounded grains included in calcite.

The mineral abbreviations used in figures are those recommended by WHITNEY & EVANS (2010).

4.2. Mineral chemistry *in situ*

Representative electron microprobe analyses of calcite and dolomite are listed in Table 1. Chemical formulae for calcite were calculated on the basis of 1 $[CO_3]^{2-}$ and those for dolomite on 2 $[CO_3]^{2-}$. The total Fe was determined as FeO. Whereas the Fe content in calcite is almost negligible, varying from 0.000 to 0.004 pfu, its content in dolomite is slightly higher, extending from 0.007 to 0.021 pfu. Calcite generally has the

Table 1. Electron microprobe analyses of representative calcite and dolomite.

Mineral	Calcite									Dolomite					
Analysis	MG 10-11	MG 10-16	MG 10-22	MG 10-35	MG 10-51	MG 10-55	MG 11-2	MG 11-12	MG 11-27	MG 10-34	MG 10-36	MG 10-50	MG 10-54	MG 11-11	MG 11-26
apfu															
Ca	0.958	0.969	0.964	0.969	0.967	0.972	0.953	0.960	0.971	1.083	1.060	1.084	1.075	1.076	1.040
Mg	0.039	0.029	0.032	0.029	0.032	0.026	0.046	0.039	0.028	0.901	0.918	0.901	0.910	0.916	0.948
Fe^{2+}	0.003	0.002	0.004	0.002	0.001	0.002	0.000	0.001	0.001	0.015	0.021	0.016	0.014	0.007	0.013
Mn	0.000	0.000	0.000	0.000	0.000	0.000	0.000	0.000	0.000	0.001	0.000	0.000	0.002	0.001	0.000
Σ	1.000	1.000	1.000	1.000	1.000	1.000	0.999	1.000	1.000	2.000	1.999	2.001	2.001	2.000	2.001
$^1X_{Mg}$	0.039	0.029	0.032	0.029	0.032	0.026	0.046	0.039	0.028	0.451	0.459	0.450	0.455	0.458	0.474
^2T (°C)	487	443	457	443	457	426	514	487	430						

Cation proportion were calculated on the basis of 1 $[CO_3]^{2-}$ for calcite and 2 $[CO_3]^{2-}$ for dolomite.

[1] $X_{Mg} = Mg/(Ca + Mg + Fe)$

[2] temperatures are determinated using the calcite-dolomite solvus geothermometer of GOLDSMITH & NEWTON (1969)

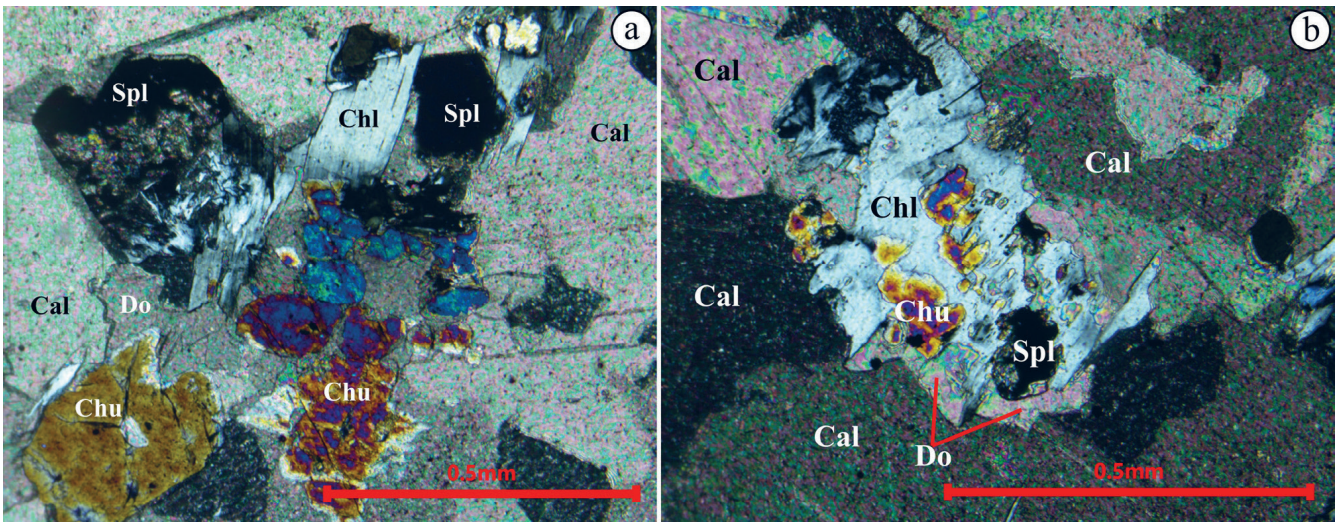

Figure 12. Photomicrographs of the common mineral assemblage in calcite marble consisting of spinel (Spl), clinohumite (Chu), calcite (Cal), chlorite (Chl) and dolomite (Do), which is consistent with the retrograde reaction Chl + Do = Spl + Chu + Cal: **a** replacement of spinel (Spl), clinohumite (Chu) and calcite (Cal) by chlorite (Chl) and dolomite (Do); **b** restites of clinohumite (Chu) and spinel (Spl) in a coarse chlorite (Chl) flake with dolomite (Do) developed at the rims of the silicate cluster.

Table 2. Electron microprobe analyses of representative forsterite.

Mineral	forsterite					
Analysis	MG 10-19	MG 10-24	MG 10-48	MG 11-1	MG 11-10	MG 11-24
wt. %						
SiO_2	42.47	42.00	42.64	43.17	42.82	43.39
TiO_2	0.01	0.05	0.00	0.00	0.02	0.00
Al_2O_3	0.00	0.01	0.00	0.00	0.01	0.00
Cr_2O_3	0.05	0.00	0.00	0.00	0.02	0.00
FeO	3.68	4.75	4.11	1.59	2.09	2.29
MnO	0.05	0.01	0.05	0.00	0.07	0.05
MgO	53.59	52.74	53.54	55.36	55.05	55.00
CaO	0.16	0.06	0.05	0.11	0.06	0.03
Σ	100.01	99.62	100.39	100.23	100.14	100.76
apfu						
Si	1.010	1.007	1.011	1.014	1.010	1.016
Ti	0.000	0.001	0.000	0.000	0.000	0.000
Al	0.000	0.000	0.000	0.000	0.000	0.000
Cr	0.001	0.000	0.000	0.000	0.000	0.000
Fe^{2+}	0.073	0.095	0.081	0.031	0.041	0.045
Mn	0.001	0.000	0.001	0.000	0.001	0.001
Mg	1.900	1.886	1.893	1.938	1.935	1.920
Ca	0.004	0.002	0.001	0.003	0.002	0.001
Σ	2.989	2.991	2.987	2.986	2.989	2.983
X_{Mg}[1]	0.963	0.952	0.959	0.984	0.979	0.977

Chemical formulas were calculated on the basis of 4 oxygens, assuming all iron as Fe^{2+}
[1]$X_{Mg} = Mg/(Mg + Fe)$

X_{Mg} value, defined as $X_{Mg} = Mg/(Ca + Mg + Fe)$, in the range of 0.026 and 0.046, indicating chemical heterogeneity. As expected, dolomite grains display higher a X_{Mg} value (0.450 to 0.474). The Mn content in calcite is below the detection limit and in dolomite is very low varying between 0.000 and 0.002 pfu.

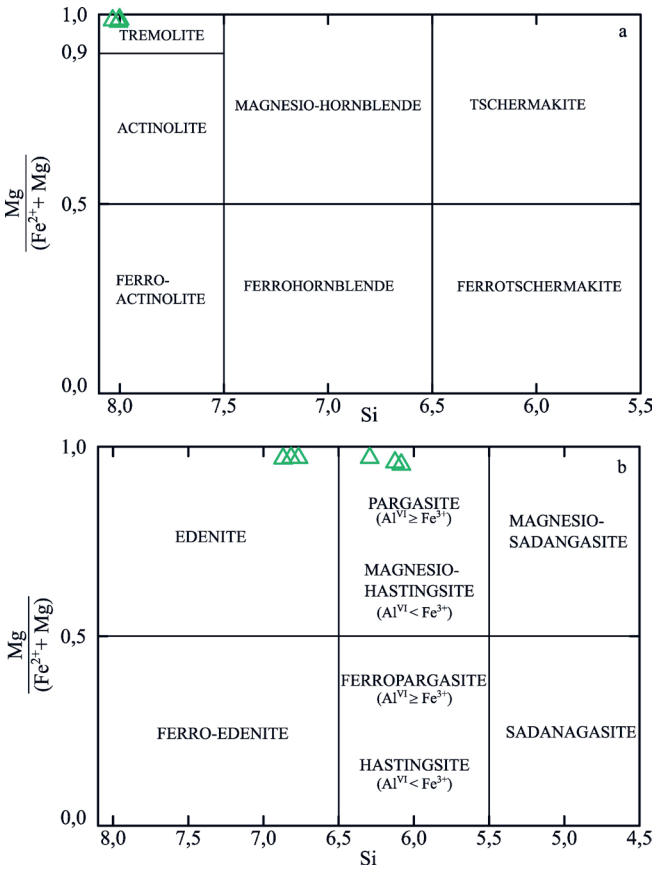

Figure 13. The classification of amphiboles according to LEAKE (1997).

The chemistry of forsterite is given in Table 2. Its chemical formulae were calculated on the basis of 4 oxygen, assuming all iron as Fe^{2+}. Olivine is strongly forsteritic having a high Mg content (1.877 – 1.940 pfu) and a low Fe content (0.032 – 0.100 pfu). The X_{Mg} value, defined as $X_{Mg} = Mg/(Mg + Fe)$, varies between 0.95 and 0.98. The Mn (0.000 – 0.003 pfu), Ca (0.000 – 0.004 pfu) and Ti content (0.000 – 0.005 pfu) in olivine are negligible.

The compositions of amphiboles are displayed in Table 3. Their chemical formulae were calculated on the basis of 23 oxygens and 13 cations, excluding Ca, Na and K and assuming all iron as Fe^{2+}. The classification of amphiboles according to LEAKE (1997) is given in Figure 13. The analyses reveal that three different amphiboles occur in studied marbles, those of pargasitic, edenitic and tremolitic compositions. Pargasite occurs as isolated coarse euhedral prismatic grains and displays compositional zonation from a pargasitic core (Table 3, analyses: MG 10-2, MG 10-5, MG 10-38) through edenite (Table 3, analyses: MG 10-3, MG 10-4, MG 10-8) to a very narrow tremolitic rim. However, amphibole occurring in the mineral assemblage with forsterite, usually as needle aggregates replacing forsterite, is solely tremolitic (Table 3, analyses: MG 10-26, MG 10-31, MG 10-52). A pargasite core is characterised by higher Al (2.370 – 2.594 pfu) and Ti content (0.154 – 0.262 pfu) in comparison to edenite (Al = 1.582.1.628 pfu; Ti = 0.109 – 0.149 pfu) and tremolite (Al = 0.045 – 0.055 pfu; Ti = 0.003.0.006 pfu). Total alkali (K + Na) content decreases from pargasite (0.792 – 0.873) through edenite (0.565 – 0.664) to tremolite (0.036 – 0.055). The F content in pargasite (0.185 –

Table 3. Electron microprobe analyses of representative amphiboles.

Mineral	pargasite			edenite			tremolite		
Analysis	MG 10-2	MG 10-5	MG 10-38	MG 10-3	MG 10-4	MG 10-8	MG 10-26	MG 10-31	MG 10-52
wt. %									
SiO_2	42.79	43.15	44.84	48.57	48.86	49.49	58.96	59.04	58.80
TiO_2	2.45	1.67	1.46	1.42	1.28	1.04	0.06	0.06	0.03
Al_2O_3	15.19	15.51	14.33	9.88	9.90	9.67	0.29	0.34	0.28
Cr_2O_3	0.01	0.02	0.01	0.02	0.00	0.00	0.02	0.05	0.04
FeO	1.64	1.43	1.07	1.14	1.11	1.20	0.69	0.83	0.58
MnO	0.02	0.04	0.00	0.00	0.03	0.01	0.00	0.00	0.04
MgO	18.46	18.56	19.39	20.84	20.62	20.78	23.80	23.92	24.05
CaO	13.59	13.63	13.53	13.71	13.66	13.78	13.80	13.93	14.08
Na_2O	2.86	2.80	2.81	2.10	2.27	2.00	0.17	0.20	0.12
K_2O	0.38	0.56	0.42	0.23	0.29	0.15	0.27	0.14	0.02
F	0.67	1.02	0.42	0.83	0.42	0.82	0.27	0.14	0.31
H_2O	1.79	1.63	1.94	1.76	1.95	1.77	2.07	2.14	2.06
Σ	99.85	100.02	100.22	100.50	100.39	100.71	100.40	100.79	100.41
F = O	0.28	0.43	0.18	0.35	0.18	0.34	0.11	0.06	0.13
Σ	99.57	99.59	100.04	100.15	100.21	100.37	100.29	100.73	100.28
apfu									
Si	6.084	6.125	6.293	6.767	6.816	6.869	8.034	8.006	8.001
Ti	0.262	0.178	0.154	0.149	0.134	0.109	0.006	0.006	0.003
Al	2.545	2.594	2.370	1.622	1.628	1.582	0.047	0.055	0.045
Cr	0.001	0.002	0.002	0.002	0.000	0.000	0.003	0.005	0.004
Fe^{2+}	0.195	0.170	0.125	0.133	0.130	0.139	0.078	0.094	0.066
Mn	0.002	0.005	0.000	0.000	0.004	0.002	0.000	0.000	0.004
Mg	3.911	3.927	4.056	4.327	4.288	4.299	4.832	4.835	4.878
Ca	2.070	2.073	2.035	2.046	2.041	2.049	2.014	2.024	2.053
Na	0.788	0.771	0.764	0.567	0.613	0.539	0.046	0.054	0.032
K	0.070	0.102	0.028	0.042	0.051	0.026	0.000	0.001	0.004
F	0.299	0.457	0.185	0.367	0.184	0.359	0.116	0.061	0.134
OH	1.701	1.543	1.815	1.633	1.816	1.641	1.884	1.939	1.866

Chemical formulas were calculated on the basis of 23 oxygens and 13 cations excluding Ca, Na and K and assuming all iron as Fe^{2+}

0.457 pfu) and edenite (0.184 – 0.367 pfu) is similar, but lower in tremolite (0.061 – 0.134 pfu). The Fe content is generally low in all amphiboles, but it is the highest in pargasite (0.125 – 0.195 pfu), lower in edenite (0.130 – 0.139 pfu) and the lowest in tremolite (0.066 – 0.094 pfu).

Representative electron microprobe analyses of clinohumite are shown in Table 4. Its chemical formulae are calculated on the basis of 13 oxygen, assuming all iron as Fe^{2+}. The Fe content in clinohumite is in the range of 0.145 to 0.415 pfu and X_{Mg} value from 0.95 to 0.98. The Ti content is quite variable, from 0.070 pfu in mineral assemblages with phlogopite (Table 6; analyses MG 10-43, MG 10-43; MG 10-49) to 0.325 pfu in mineral assemblages with amphibole. A weak Ti zonation pattern can be observed in clinohumite with the highest concentration of Ti in the core and the lower Ti values in the rest of the grain. The X_F value in clinohumite, defined as F/(F + OH), varies from 0.32 to 0.57. The Mn content, found to be in the range from 0.000 to 0.007 pfu, is negligible.

The compositions of spinel and ilmenite are shown in Table 5. The chemical formulae for spinel are calculated on the basis of 3 cations and 4 oxygens, and for ilmenite on the basis of 2 cations and 3 oxygens. Spinel is almost pure Mg-Al spinel characterised by a high X_{Mg} value (0.93 – 0.96) and by a Zn content varying between 0.003 and 0.013 pfu. In contrast to all other minerals in the marbles, spinel contains a minor amount of Fe^{3+} (up to 0.19 pfu; Table 5). It is evident from the chemical analyses that two different types of ilmenite occur in analysed marbles. Ilmenite appearing as rounded opaque grains in pargasite corresponds to pure ilmenite with a Mg content of only 0.004 pfu (Table 5; analyse MG 10-6). But ilmenite observed as rare inclusions in spinel or in chlorite replacing spinel ± clinohumite is geikielite. This Mg-rich ilmenite contains very high Ti (1.026 pfu) and Mg content (0.725 pfu), but low Fe content (0.244 pfu), as shown in Table 5 (analysis MG 11-31). The absence of any Cr content in the studied Mg-rich ilmenite distinguishes it from the Mg-rich ilmenite usually occurring in kimberlites and lamproites (GIERÉ, 1987).

The chemistry of talc is displayed in Table 6 and its chemical formulae were calculated on the basis of 11 oxygens. A small amount of Fe (0.046 – 0.089 pfu) substitutes for Mg and a minute quantity of Al (0.020 – 0.064) replaces Si. Talc occurs solely as a replacement in the mineral assemblages with forsterite.

Table 4. Electron microprobe analyses of representative clinohumites.

Mineral	clinohumite									
Analysis	MG 10-15	MG 10-42	MG 10-43	MG 10-49	MG 10-58	Mg 11-5	MG 11-19	MG 11-21	MG 11-22	MG 11-23
wt. %										
SiO_2	37.07	37.44	37.37	37.51	37.42	37.23	37.47	37.26	37.26	37.58
TiO_2	4.05	1.96	0.96	0.88	3.39	3.23	2.51	3.37	2.05	2.32
Al_2O_3	0.01	0.00	0.00	0.00	0.00	0.01	0.03	0.01	0.00	0.00
Cr_2O_3	0.00	0.02	0.07	0.01	0.00	0.02	0.00	0.04	0.05	0.01
FeO	4.64	4.61	4.40	4.79	2.58	1.67	2.48	2.07	1.99	1.64
MnO	0.00	0.07	0.00	0.00	0.00	0.01	0.05	0.02	0.01	0.05
MgO	52.05	53.00	54.27	53.67	54.38	54.82	54.61	54.74	55.63	55.61
CaO	0.13	0.03	0.05	0.12	0.04	0.03	0.02	0.00	0.03	0.01
F	1.30	2.35	3.16	2.81	2.09	2.01	2.01	1.84	2.62	2.65
H_2O	2.58	2.52	2.26	2.59	2.20	2.35	2.66	2.46	2.33	2.17
Σ	101.83	102.00	102.54	102.38	102.10	101.38	101.84	101.81	101.97	102.04
F = O	0.55	0.99	1.33	1.18	0.88	0.84	0.84	0.77	1.10	1.12
Σ	101.28	101.01	101.21	101.19	101.22	100.54	100.99	101.03	100.97	100.92
apfu										
Si	3.958	3.993	3.967	3.987	3.948	3.940	3.960	3.932	3.922	3.951
Ti	0.325	0.157	0.077	0.070	0.269	0.257	0.199	0.267	0.162	0.184
Al	0.001	0.000	0.000	0.000	0.000	0.001	0.004	0.002	0.000	0.000
Cr	0.000	0.002	0.060	0.001	0.000	0.002	0.000	0.003	0.004	0.001
Fe^{2+}	0.415	0.411	0.390	0.426	0.227	0.148	0.219	0.182	0.175	0.145
Mn	0.000	0.007	0.000	0.000	0.000	0.001	0.005	0.002	0.001	0.004
Mg	8.284	8.424	8.565	8.502	8.550	8.647	8.603	8.608	8.729	8.714
Ca	0.015	0.004	0.005	0.014	0.005	0.003	0.002	0.001	0.004	0.002
F	0.439	0.792	1.058	0.945	0.699	0.671	0.670	0.614	0.872	0.882
OH	0.920	0.896	0.799	0.918	0.775	0.828	0.938	0.866	0.820	0.762
$^1X_{Mg}$	0.95	0.95	0.96	0.95	0.97	0.98	0.98	0.98	0.98	0.98
^2X_F	0.32	0.47	0.57	0.51	0.47	0.45	0.42	0.41	0.52	0.54

Chemical formulas were calculated on the basis of 13 oxygens, assuming all iron as Fe^{2+}

$^1X_{Mg} = Mg/(Mg+Fe)$

$^2X_F = F/(F+OH)$

The chemical compositions of chlorites are also shown in Table 6. Their chemical formulae were calculated on the basis of 20 cations and 28 oxygens per formula unit. The Si values vary from 5.688 to 6.730 pfu, the Si/Al ratio is in the range from 1.18 to 2.19, whereas Al in the tetrahedral site (Al^{IV}) show significant variability, ranging from 1.27 to 2.31 pfu. The X_{Mg} value in all chlorites is extremely high, varying from 0.96 to 1.00. Classification of chlorites based on the amounts of Si and Fe in structural formulae according to the diagram of HEY (1954) is given in Figure 14. There are differences in the chemical composition of chlorites depending on the mineral assemblages in which they occur. Chlorite occurring in mineral assemblage with tremolite, serpentine, talc and dolomite replacing forsterite (Fig. 5a; analyses MG 10-37, MG 10-39, MG-10-57 in Table 6) is penninite in composition, whereas chlorite replacing spinel ± clinohumite in mineral assemblages is clinochlore (Fig. 12a, b; analyses MG 11-14, MG 11-20, MG 11-52 in Table 6).

Generally, low iron concentrations are typical for all analysed minerals in studied marbles.

4.3. Compositional maps of characteristic mineral assemblages

With the aim of better visualisation of the minerals in the mineral assemblages and recognition of any possible inhomogeneity within the minerals, the analyses of spatial distribution of specific chemical elements for all mineral assemblages of interest were performed and are shown in Figures 15, 16, 17 and 18. The elemental distribution maps were obtained from 2 x 2 mm sections for all mineral assemblages, excluding those consisting of calcite, dolomite, forsterite, serpentine and tremolite in sample MG 11, shown in Figure 17. There, the maps were obtained from 3 x 3 mm sections.

Elemental distribution characteristics for Ca, Mg and Al in a mineral assemblage consisting of calcite, dolomite, forsterite, serpentine, tremolite, pargasite and chlorite in sample MG 10 are shown in Figure 15. The lowest concentrations of Ca are present in mineral phases denoted in a black colour (forsterite, chlorite) and the highest concentrations in the mineral phase expressed in light blue (calcite) as shown in Figure 15a. The blue colour in the same Figure refers to the presence of pargasite and serpentine, the green colour to tremolite, whereas the red coloured area corresponds to dolomite. This elemental map clearly highlights the difference between calcite and dolomite. Calcite greatly exceeds dolomite, which is predominantly associated with the silicate mineral assemblage, commonly occurring at the forsterite rims. The concentrations of Mg in minerals are presented in Figure 15b. The grey and white colour refers to the presence of calcite. This elemental map clearly shows the inhomogeneous distri-

Table 5. Electron microprobe analyses of representative spinel and ilmenite.

Mineral	spinel							ilmenite	
Analysis	MG 11-46	MG 11-47	MG 11-48	MG 11-50	Mg 11-51	MG 11-54	MG 11-55	MG 10-6	MG 11-31
wt. %									
TiO_2	n.a.	n.a.	n.a.	n.a.	n.a.	n.a.	n.a.	53.42	64.01
Al_2O_3	69.68	69.44	69.52	69.57	69.77	69.12	69.57	n.a.	n.a.
Cr_2O_3	0.01	0.00	0.01	0.05	0.02	0.00	0.00	0.00	0.00
Fe_2O_3	0.58	0.64	0.81	0.77	0.00	0.77	1.09	0.00	0.00
FeO	1.72	2.45	2.51	2.07	3.30	2.77	1.75	44.21	13.65
MnO	0.00	0.00	0.00	0.00	0.01	0.00	0.02	0.17	0.23
ZnO	0.28	0.22	0.58	0.17	0.50	0.70	0.11	n.a.	n.a.
MgO	26.59	26.05	25.95	26.46	25.34	25.55	26.72	1.68	22.82
CaO	0.00	0.10	0.06	0.01	0.07	0.10	0.01	n.a.	n.a.
Σ	98.86	98.90	99.44	99.10	99.01	99.01	99.27	99.48	100.71
apfu									
Ti	n.a.	n.a.	n.a.	n.a.	n.a.	n.a.	n.a.	1.003	1.026
Al	1.989	1.988	1.985	1.985	2.002	1.986	1.980	n.a.	n.a.
Cr	0.000	0.000	0.000	0.001	0.000	0.000	0.000	0.000	0.000
Fe^{3+}	0.011	0.012	0.015	0.014	0.000	0.014	0.019	0.000	0.000
Fe^{2+}	0.035	0.050	0.051	0.042	0.067	0.056	0.035	0.923	0.244
Mn	0.000	0.000	0.000	0.000	0.000	0.000	0.000	0.004	0.004
Zn	0.005	0.004	0.010	0.003	0.009	0.013	0.002	n.a.	n.a.
Mg	0.960	0.944	0.937	0.955	0.919	0.929	0.962	0.063	0.725
Ca	0.000	0.003	0.002	0.000	0.002	0.003	0.000	n.a.	n.a.
$^1X_{Mg}$	0.96	0.95	0.95	0.96	0.93	0.94	0.96		

Chemical formulas were calculated on the basis of 3 cations and 4 oxygens for spinel, and 2 cations and 3 oxygens for ilmenite
$^1X_{Mg} = Mg/(Mg+Fe^{2+})$
n.a. = not analysed

bution of Mg in calcite. The blue colour represents dolomite and the green is tremolite. The higher Mg concentrations are shown in yellow for pargasite, serpentine and chlorite, whereas red denotes the highest Mg concentrations being typical of forsterite. The distribution of Al in this mineral assemblage is shown in Figure 15c. There is no Al content in calcite, dolomite and forsterite, which is displayed as a light blue colour. The highest Al concentrations are denoted in red and refer to the

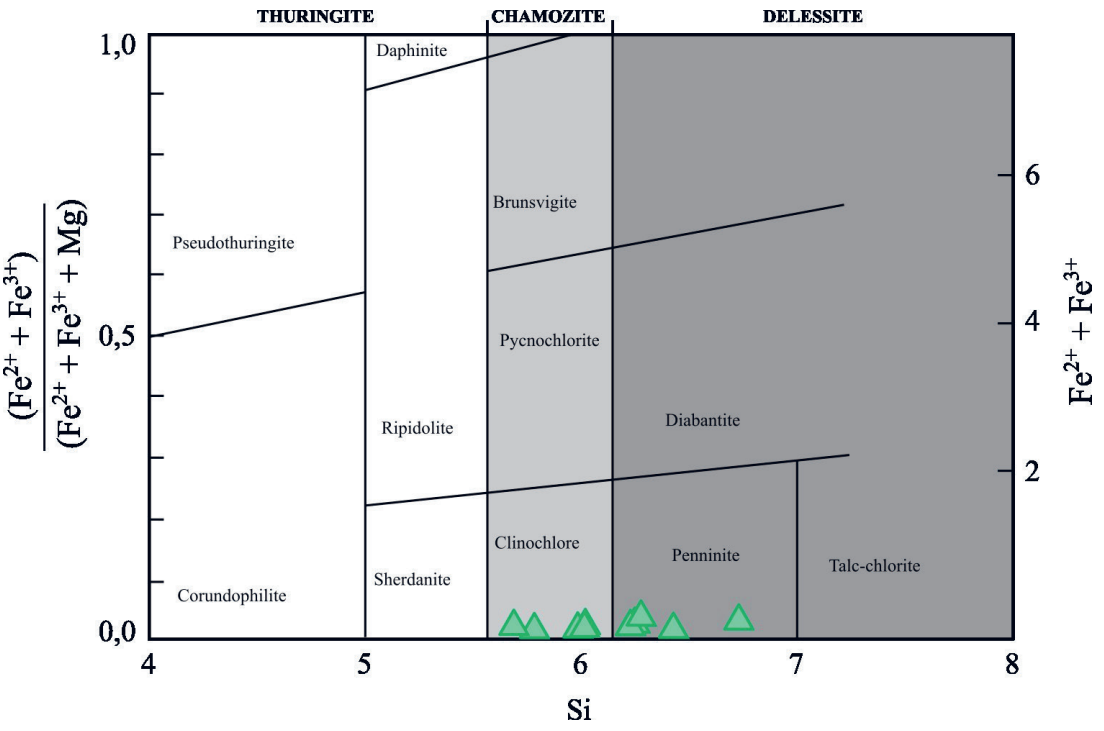

Figure 14. Classification of chlorites based on the amounts of Si, Fe and Mg in the structural formulae according to HEY (1954).

Table 6. Electron microprobe analyses of representative talc and chlorite.

Mineral	talc		chlorite									
Analysis	MG 10-80	MG 10-85	MG 10-12	MG 10-37	MG 10-39	Mg 10-57	MG 10-64	MG 10-18	MG 11-14	MG 11-20	MG 11-41	MG 11-52
wt. %												
SiO_2	62.56	63.82	35.48	32.80	32.97	33.92	32.82	31.65	30.44	31.38	31.52	30.04
TiO_2	0.02	0.00	0.05	0.09	0.13	0.03	0.11	0.07	0.06	0.16	0.12	0.05
Al_2O_3	0.49	0.27	13.76	17.40	17.46	16.22	18.15	19.50	22.18	20.43	20.21	21.58
Cr_2O_3	0.00	0.02	0.05	0.06	0.00	0.00	0.05	0.07	0.01	0.06	0.00	0.00
FeO	1.39	1.06	1.89	0.00	1.27	0.97	2.13	1.33	0.88	0.95	1.02	1.23
MnO	0.02	0.04	0.03	1.51	0.00	0.03	0.05	0.00	0.00	0.01	0.05	0.00
MgO	29.60	30.45	34.88	33.67	34.28	34.42	32.22	33.11	32.11	32.46	32.49	32.83
CaO	0.09	0.07	0.08	0.04	0.08	0.28	0.05	0.02	0.01	0.04	0.05	0.10
Na_2O	0.07	0.09	0.00	0.03	0.00	0.01	0.04	0.00	0.02	0.00	0.00	0.00
K_2O	0.01	0.02	0.02	0.00	0.01	0.01	0.20	0.00	0.00	0.01	0.00	0.02
H_2O	4.67	4.76	12.65	12.59	12.70	12.66	12.54	12.61	12.63	12.58	12.57	12.56
Σ	98.92	100.60	98.89	98.19	98.90	98.55	98.36	98.36	98.34	98.08	98.03	98.41
apfu												
Si	4.013	4.020	6.730	6.249	6.228	6.427	6.277	6.019	5.783	5.984	6.016	5.688
Ti	0.001	0.000	0.007	0.012	0.018	0.005	0.016	0.010	0.009	0.022	0.017	0.007
Al	0.037	0.020	3.077	3.908	3.887	3.623	4.089	4.369	4.967	4.592	4.546	4.817
Cr	0.000	0.001	0.000	0.009	0.000	0.000	0.008	0.002	0.002	0.009	0.000	0.000
Fe^{2+}	0.074	0.056	0.299	0.240	0.200	0.154	0.341	0.212	0.139	0.151	0.163	0.195
Mn	0.001	0.002	0.005	0.000	0.000	0.005	0.008	0.000	0.140	0.151	0.000	0.000
Mg	2.831	2.859	9.860	9.563	9.650	9.722	9.185	9.383	9.091	9.228	9.241	9,265
Ca	0.006	0.005	0.016	0.008	0.016	0.057	0.001	0.004	0.002	0.008	0.009	0.021
Na	0.009	0.011	0.002	0.010	0.000	0.005	0.016	0.000	0.007	0.000	0.000	0.002
K	0.001	0.002	0.005	0.000	0.017	0.003	0.050	0.000	0.000	0.003	0.000	0.006
OH	2.000	2.000	16.000	16.000	16.000	16.000	16.000	16.000	16.000	16.000	16.000	16.000
$^1X_{Mg}$	0.97	0.98	0.97	0.98	0.98	0.98	0.96	0.98	0.98	0.98	0.98	1.00
Si/Al			2.19	1.60	1.60	1.77	1.54	1.38	1.16	1.30	1.32	1.18
Al^{IV}			1.27	1.75	1.77	1.57	1.72	1.98	2.22	2.02	1.98	2.31

Chemical formulas were calculated on the basis of 11 oxygens for talc, and on the basis of 20 cations and 28 oxygens for chlorite
$^1X_{Mg}$ = Mg/(Mg+Fe)

presence of pargasite and chlorite. Due to the subtle variations in Al concentrations in pargasite and chlorite, the yellow colour refers to these minerals too. The Al content cannot be used for differentiation between these two minerals. The lowest concentration of Al is present in serpentine and partly in tremolite, which is marked in black. Additionally, the tremolite containing a little bit more Al shows as a blue colour, whereas the occurrence of a small quantity of green denotes the transition of a tremolite to edenite composition. The distribution of Al demonstrates that tremolite occurs solely at the rims of silicate clusters.

Elemental distribution characteristics for Ca, Al and Si in the mineral assemblage consisting of calcite, euhedral prismatic amphibole and smaller forsterite grain in sample MG 10 are shown in Figure 16. The lowest Ca content, denoted in black, have forsterite and chlorite replacing amphibole along its cracks (Fig. 16a). A higher Ca content corresponding to a green colour is typical for amphibole, independent of amphibole type. The small patchy yellow domains within amphibole grain point to a slightly higher Ca content and variation in its composition. The red colour refers to the presence of dolomite along the rims of forsterite, whereas the light blue colour corresponds to calcite. The distribution of Al in this mineral assemblage is shown in Figure 16b. Calcite, dolomite and forsterite do not contain Al, and they are therefore represented in a light blue colour. The black colour denotes serpentine and tremolite. Higher Al content, expressed in blue, characterises edenite, whereas chlorite shows still higher Al concentrations, displayed in green. The highest Al concentrations, denoted in yellow and red are present in pargasite, but also in chlorite, since the Al content in these two minerals shows variations. The distribution of Si in this mineral assemblage is presented in Figure 16c. The light blue colour denotes the presence of calcite and dolomite. Higher Si concentration has chlorite, denoted in black. The green colour refers to the occurrence of forsterite and pargasite. Due to the variation in Si content, pargasite is also marked in yellow, as is serpentine. The highest Si concentrations are typical for edenite and tremolite. The elemental maps for Ca, Al and Si highlighted high grade of chemical variations in the studied amphibole grain.

Elemental distribution characteristics for Ca, Mg and Si in the mineral assemblage consisting of calcite, dolomite, forsterite, serpentine and tremolite in sample MG 11 are shown

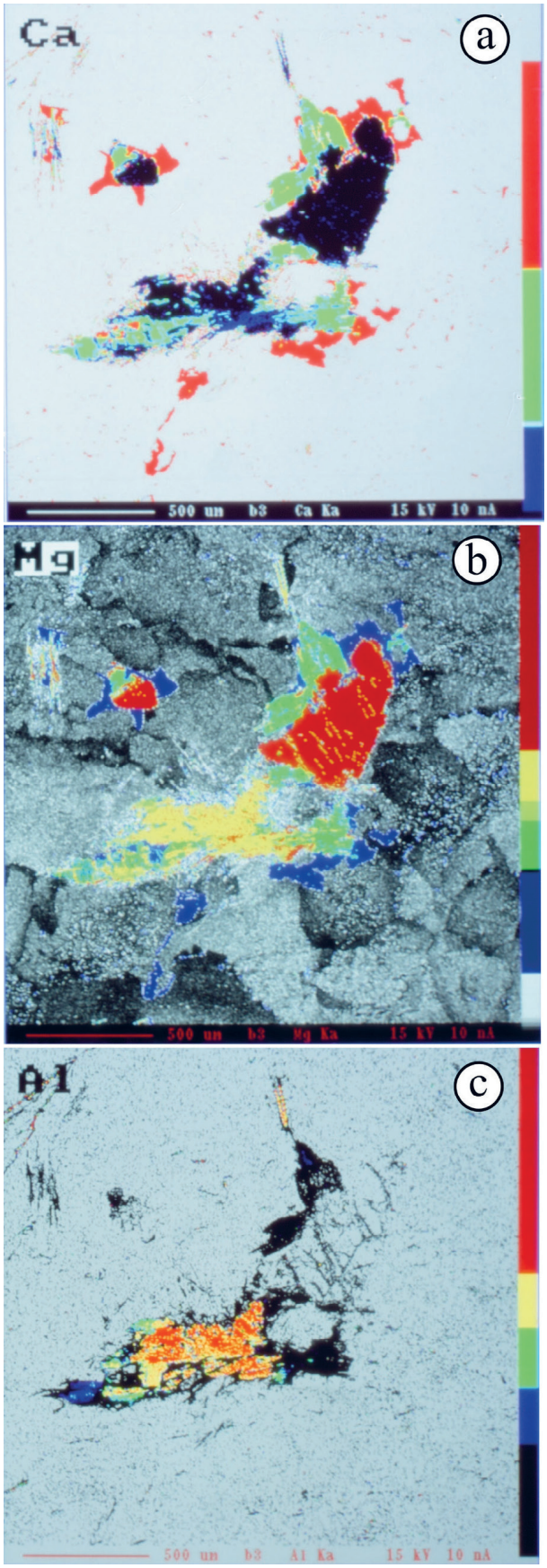

Figure 15. Elemental distribution maps for Ca, Mg and Al in the mineral assemblage consisting of calcite, dolomite, forsterite, serpentine, tremolite, pargasite and chlorite in sample MG 10. Elemental concentration steps from low to high display the colours: **a** for Ca from black, blue, green, red and light blue in order; **b** for Mg from grey, white, blue, green, yellow and red in order; **c** for Al from light blue, black, blue, green, yellow and red in order.

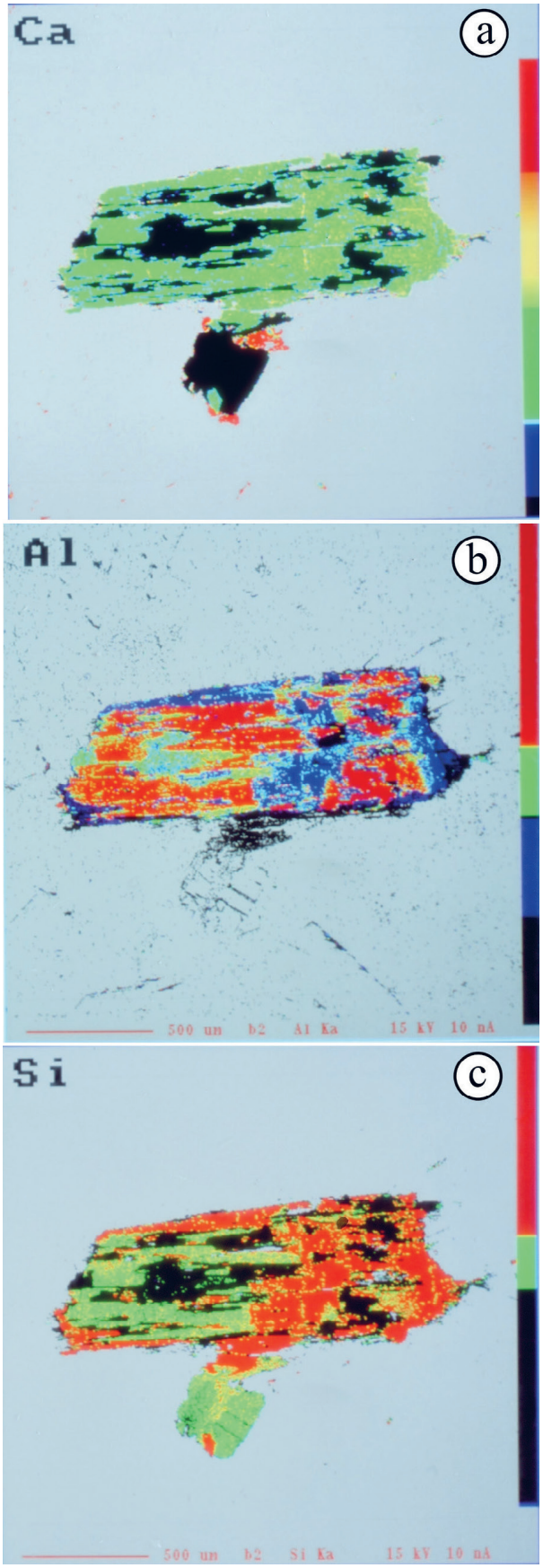

Figure 16. Elemental distribution maps for Ca, Al and Si in the mineral assemblage consisting of calcite, euhedral prismatic amphibole and smaller forsterite grains in sample MG 10. Elemental concentration steps from low to high display the colours: **a** for Ca from black, blue, green, yellow, red and light blue in order; **b** for Al from light blue, black, blue, green, yellow and red in order; **c** for Si from light blue, black, green, yellow and red in order.

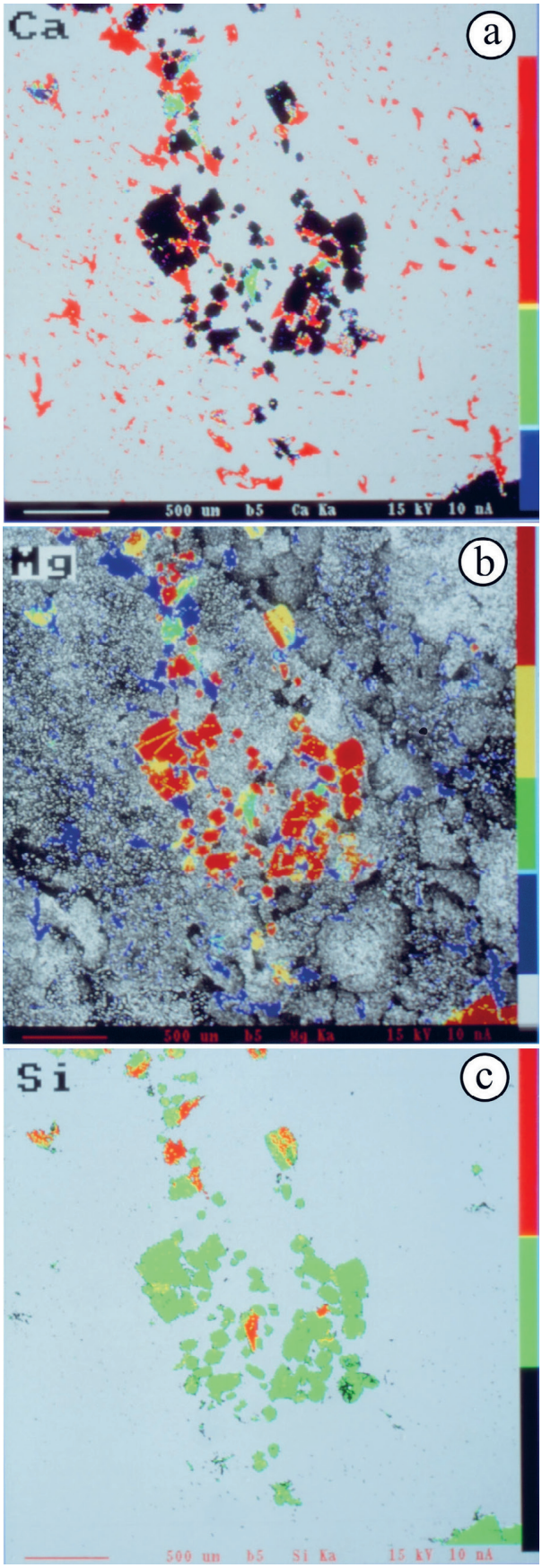

Figure 17. Elemental distribution maps for Ca, Mg and Si in the mineral assemblage consisting of calcite, dolomite, forsterite, serpentine and tremolite in sample MG 11. Elemental concentration steps from low to high display the colours: **a** for Ca from black, blue, green, yellow, red and light blue in order; **b** for Mg from grey, white, blue, green, yellow and red in order; **c** for Si from light blue, black, green, yellow and red in order.

in Figure 17. The distribution of Ca in this mineral assemblage is visible in Figure 17a. Forsterite, occurring as anhedral grains of different sizes contains no Ca, therefore is marked in black, whereas blue denotes the presence of serpentine. The higher Ca concentrations are typical for tremolite, which is denoted in green. The light blue colour refers to the presence of calcite, and red corresponds to dolomite, which is, in this sample, more abundant than in sample MG 10. The elemental distribution map for Ca clearly demonstrates that dolomite occurs as tiny, almost invisible exsolution patches in calcite, or as coarser anhedral grains along the calcite grain boundaries, but the coarsest dolomite grains are associated with silicate mineral assemblages. The distribution of Mg in this mineral assemblage is shown in Figure 17b. The calcite contains the lowest Mg content, although variable, and is therefore presented in grey and white colours. The cores of some calcite grains seem to have higher Mg concentration than the rims. Dolomite is denoted in blue. Tremolite having higher Mg content is presented in green and serpentine in yellow. Forsterite has the highest Mg concentration in this mineral assemblage and therefore is marked in red. The distribution of Si in this mineral assemblage is presented in Figure 17c. Calcite and dolomite contain no Si and therefore are presented in the light blue colour. Forsterite is denoted in green, and the yellow colour refers to a small quantity of serpentine. The highest Si content in red corresponds to tremolite. The black colour seems to denote some impurities in the thin section.

Elemental distribution characteristics for Ca, Mg, Al and Ti in the mineral assemblage consisting of calcite, dolomite, forsterite, clinohumite, chlorite and tremolite in sample MG 11 are shown in Figure 18. The distribution of Ca in this mineral assemblage is visible in Figure 18a. There is no Ca in clinohumite, forsterite and chlorite, hence they are represented in a black colour. Small amounts of green denote tremolite. Dolomite occurring on the rim of silicate clusters and finely dispersed in calcite and along its grain boundaries is marked in red. The light blue colour denoting the highest Ca concentration refers to calcite. Subtle variations in the Mg content of calcite can be distinguished by black, grey and blue colours (Fig. 18b). The higher Mg content in green colours corresponds to dolomite, whereas yellow refers to chlorite and tremolite. The orange-coloured area with the highest Mg content defines both clinohumite and forsterite. They cannot be distinguished on the basis of their Mg content, but both minerals show patchy inhomogeneous anhedral internal domains. The distribution of Al in this mineral assemblage is visible in Figure 18c. It is obvious that here, Al is present only in chlorite, what is denoted in red, and tremolite shows as yellow. The light blue colour corresponds to all the other minerals in this mineral assemblage. The green colour refers to impurities in the thin-section resulting from sample preparation. The distribution of Ti in this mineral assemblage is visible in Figure 18d. This map confirms that Ti is present only in clinohumite, which is denoted in yellow. However, within clinohumite grains, patchy, orange-coloured areas represent the highest Ti concentrations, whereas the green areas located at the rims of clinohumite grains, denoted the lowest Ti concentrations. All other minerals in this mineral assemblage are denoted in a light blue colour.

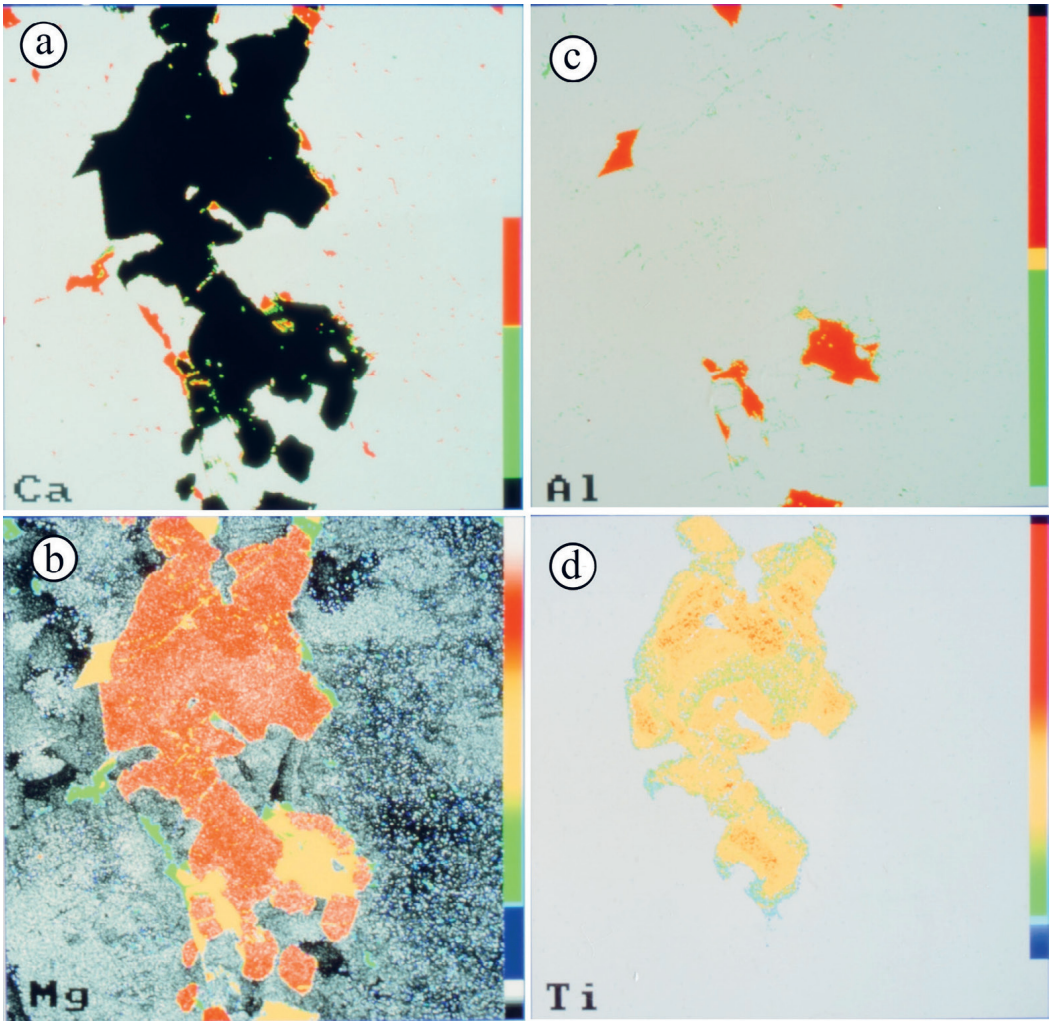

Figure 18. Elemental distribution maps for Ca, Mg, Al and Ti in the mineral assemblage consisting of calcite, dolomite, forsterite, clinohumite, chlorite and tremolite in sample MG 11. Elemental concentration steps from low to high display the colours: **a** for Ca from black, green, yellow, red and light blue in order; **b** for Mg from black, grey, white, blue, green, yellow, orange and pale orange in order; **c** for Al from light blue, green, yellow, red and black in order; **d** for Ti from light blue, blue, green, yellow, orange and black in order.

5. DISCUSSION

5.1. Solvus thermometer

The temperature dependence of Mg exchange between calcite and dolomite is generally applied for peak temperature determination in marbles in both regionally and contact metamorphosed terrains. This thermometer based on the calcite-dolomite miscibility gap has been experimentally and empirically well calibrated (GOLDSCHMITH & NEWTON, 1969; POWELL et al., 1984; ANOVITZ & ESSENE, 1987). However, care is required due to the possible resetting of temperatures during the cooling process (LETARGO et al., 1985), especially in higher grades of metamorphism where exsolution textures in calcite are present (MIZUOCHI et al., 2010).

The formulation of GOLDSCHMITH & NEWTON'S (1969) calcite-dolomite solvus thermometer was used in this study, although this formulation does not account for Fe. It is still appropriate due to the negligible Fe content in the analysed carbonates (Table 1).

The obtained temperatures are in the range between 426 ºC and 487 ºC in the sample MG 10 and between 430 ºC and 514 ºC for sample MG 11 (Table 1). Such low temperature determinations may be ascribed to retrogression and the closure temperature of Mg diffusion during uplift history, especially in light of the fact that elemental compositional

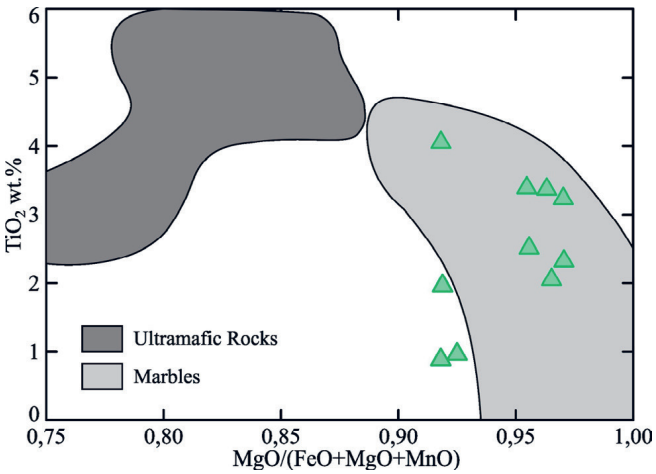

Figure 19. The comparison of clinohumite compositions in grey marbles from Mt. Moslavačka gora with other marbles worldwide in the plot of TiO_2 vs Mg/(FeO + MgO + MnO) after RIOS et al. (2015). Clinohumites of Mt. Moslavačka gora are marked by green triangles.

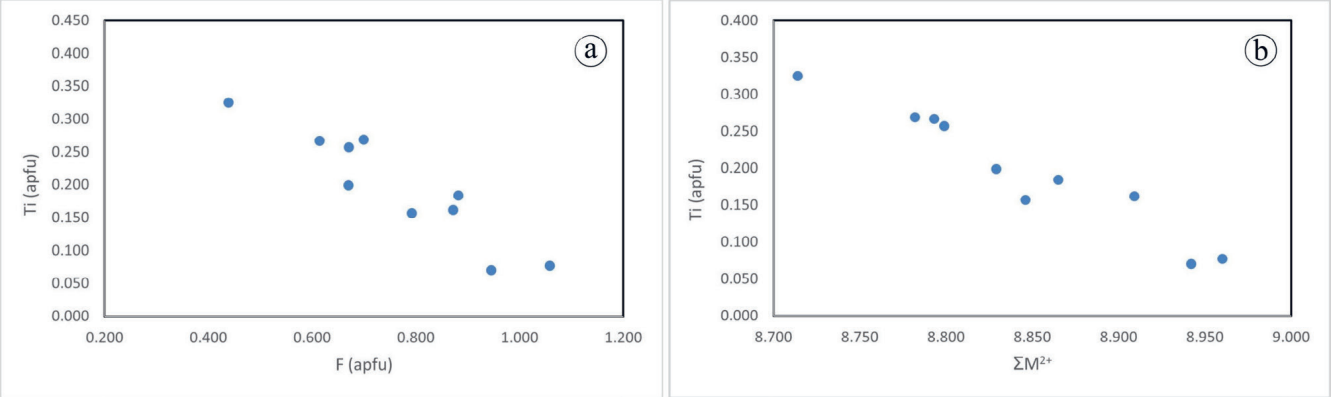

Figure 20. The usually expected substitution (Mg, Fe) + 2 (OH, F) = Ti + 2 (O) in clinohumites is evidenced in clinohumites of Mt. Moslavačka gora too, by: **a** an inverse variation of Ti with fluorine content ($R^2 = 0.86$) and **b** an inverse variation of Ti with ΣM^{2+} ($R^2 = 0.94$) where ΣM^{2+} = Mg + Fe + Mn + Ca.

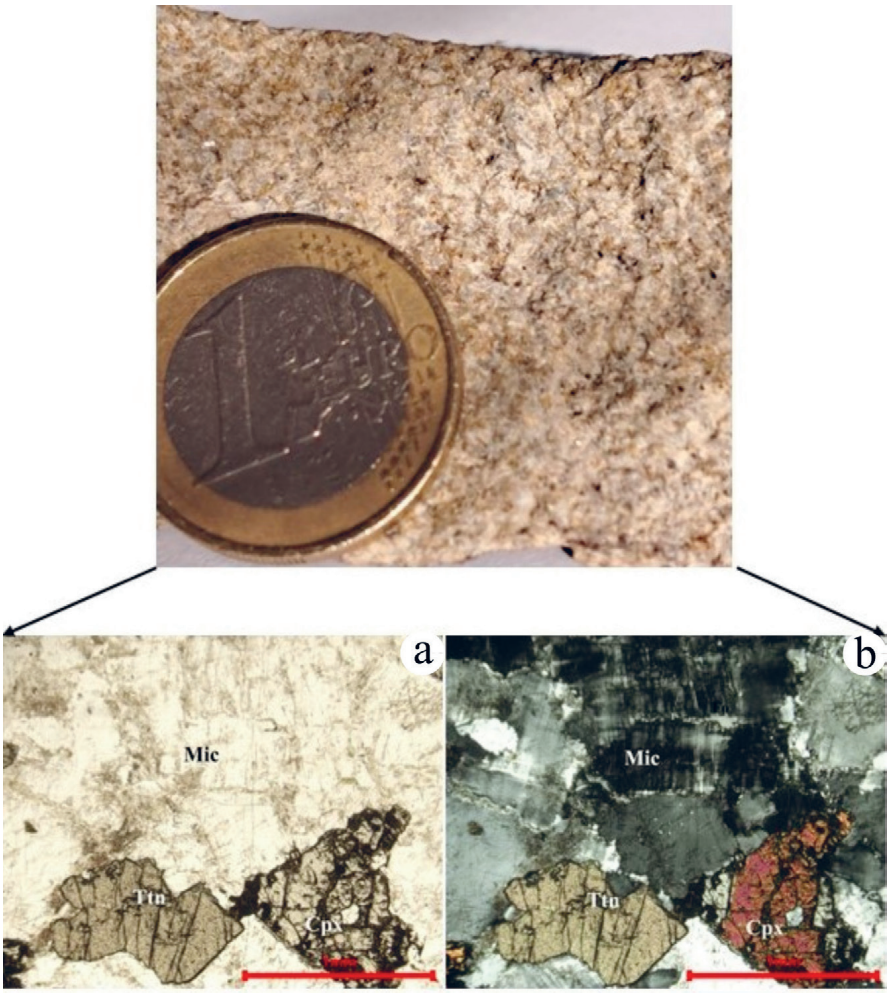

Figure 21. Light-coloured alkali feldspar syenite, composed mainly of microcline, orthoclase, diopside, slightly altered to actinolite, and titanite.

maps of mineral assemblages clearly demonstrate extensive dolomite exsolutions within the calcite grains and along calcite grain boundaries (Fig. 15).

5.2. Mineral assemblages and reactions

Careful investigations of microstructures, including petrography and compositional mapping of mineral assemblages, revealed that the granoblastic mineral assemblage consisting of calcite + dolomite + forsterite + pargasite + spinel + phlogopite + ilmenite + apatite, which corresponds to the peak metamorphic stage in the granulite facies, is overprinted by a variety of later local reactions which have not gone to completion. The clinohumite occurrence, showing high Ti (0.070 – 0.325 pfu) and F (0.614 – 1.058 pfu) contents (Table 4, Fig. 18), indicates that temperature and pressure were not the only variables controlling the mineralogy of the studied marbles but implies the presence of fluids enriched in titanium, hydroxyl and fluorine during metamorphism. Depending on mineral assemblages, seven reactions can be deduced on the basis of the textural relationships of minerals and compositional mapping.

The textural relationships in the mineral assemblages consisting of forsterite + dolomite + calcite + clinohumite (Fig. 7) clearly indicate the replacement of forsterite by clinohumite and suggest that the clinohumite was probably formed by the following decarbonation reaction:

4 forsterite + 1 dolomite + 1-nH_2O + nHF =
4 clinohumite + calcite + CO_2 (1)

The same reaction is documented in Figure 18, where small amounts of chlorite as subsequent replacement of clinohumite and some tremolite partly replacing forsterite also occur. It should be emphasized that many forsterite grains in the studied marbles are well-preserved (Fig. 6) and did not undergo reaction (1), which can either be attributed to the local absence of dolomite as a necessary reactant in this reaction or the unequal distribution of fluids in the marbles.

The relics of spinel and clinohumite in large chlorite flakes associated with dolomite (Fig. 12a, b) may be described by the retrograde reaction:

4 chlorite + 11 dolomite =
3 clinohumite + 4 spinel + 11 calcite + 11 CO_2 + 13 H_2O (2)

Chlorite also occurs in the mineral assemblage with spinel, calcite, dolomite and forsterite where it may be formed according to the following retrograde reaction:

chlorite + 2 dolomite =
3 forsterite + spinel + 2 CO_2 + 4 H_2O + 2 calcite (3)

Tremolite and dolomite commonly occur at forsterite rims (Figs. 8, 9, 15, 17) and may be ascribed to the retrograde reaction between calcite and forsterite:

1 tremolite + 11 dolomite =
8 forsterite + 13 calcite + 9 CO_2 + 1 H_2O (4)

The occurrence of talc, commonly observed at the contact between forsterite and calcite (Fig. 5a, b), or as pseudomorphs after forsterite, associated with dolomite, corresponds to the retrograde reaction:

1 talc + 5 dolomite =
4 forsterite + 5 calcite + 5 CO_2 + 1 H_2O (5)

The formation of serpentine which generally appears along olivine cracks and grain boundaries (Figs. 5a, b, 15, 17) may be explained by the following retrograde reaction:

2 serpentine = 3 forsterite + 4 H_2O + SiO_2 (6)

Serpentine also occurs in the mineral assemblage with forsterite and talc (Fig. 5a, b), representing the product of retrograde reaction between forsterite and talc:

5 serpentine = 6 forsterite + talc + 9 H_2O (7)

All the described reactions involve changes in the modal proportions of minerals: a) resorption of forsterite by clinohumite, tremolite, chlorite, serpentine and talc, b) resorption of clinohumite by chlorite and c) resorption of spinel by chlorite. Dolomite was replaced only in a decarbonation reaction (1) involving the formation of clinohumite and calcite, but dolomite growth is typical in retrograde reactions from (2) to (5). The opposite is true for calcite.

Pargasite occurs mostly as individual euhedral prismatic grains (Figs. 8, 16) and it seems that it has not been involved into the classical reactions with other minerals. Pargasite only readjusted its composition to the prevailing PT conditions that can be traced back from the tremolitic rim through edenitic to the pargasitic core (Fig. 16).

Individual flakes of phlogopite (Fig. 10) also show no reaction relationship to other mineral phases, with the exception of only one zonal phlogopite flake found in the mineral assemblage with forsterite, clinohumite, calcite and dolomite (Fig. 11). It seems that this zonal phlogopite replaces clinohumite and forsterite and most probably does not have the same origin as the other observed phlogopite flakes in the sample. The individual flakes occurring along the calcite grains (Fig. 10) may possibly have grown at the cost of dolomite.

It can be concluded, deduced from the observation of the microstructural relationships, that apatite and geikielite have not been involved in modal changes and reactions.

5.3. Significance of the occurrence of Ti-clinohumite

The studied clinohumite from Mt. Moslavačka Gora is characterized by its variable TiO_2 content (0.88 – 4.04 wt.%) as well as its changeable F content (1.30 – 3.16 wt.%), whereas X_F is in the range of 0.32 to 0.57 wt.%. Similar values have been reported for clinohumite from the impure dolomitic limestone at Ross Lake in northern Washington (RICE, 1980), and the close range of TiO_2 contents in clinohumite were also found in carbonatites from the Jacupiranga Complex in Brazil (GASPAR, 1992). The similarity of the clinohumite compositions in marbles from Mt. Moslavačka Gora with other marbles worldwide, is shown in the plot of TiO_2 vs Mg/(FeO + MgO + MnO) after RIOS et al. (2015) in Figure 19. In the clinohumites of Mt. Moslavačka Gora, there is an inverse variation of Ti with both fluorine content (R^2 = 0.86; Fig. 20a) and ΣM^{2+} (R^2 = 0.94; Fig. 20b), where ΣM^{2+} = Mg + Fe + Mn + Ca. This is consistent with the expected substitution (Mg, Fe) + 2 (OH, F) = Ti + 2 (O) in clinohumites. RICE (1980) highlighted the importance of fluorine substitution in clinohumite demonstrating that higher fluorine concentration enlarges the stability field of clinohumite to a more CO_2-rich fluid composition in the T-X_{CO2} phase diagram.

The clinohumite occurrence in marbles has usually been explained as a result of metasomatism involving the introduction of fluorinated fluids (PRADEEPKUMAR & KRISHNANATH, 1996; BOUREGHDA et al., 2023), or being associated with the internal buffering mechanism of fluorine concentration, including mineral phases such as amphiboles or phlogopite (SATISH-KUMAR & NIIMI, 1998). According to RICE (1980) the infiltration of externally derived F-rich fluids is commonly related to the contact metamorphism and intrusion of granitoid rocks, whereas the partitioning of fluorine between clinohumite, amphibole and phlogopite in isochemical reactions may occur in regional metamorphism. More recently, KARMAKAR (2021) reported about clinohumite for-

mation in forsterite marbles as a consequence of the infiltration of F- and Ti-enriched aqueous fluids associated with hydration and alteration of the mafic rocks. RIOS et al. (2015) explained the occurrence of Ti-clinohumite in skarns by the dehydration of surrounding pelitic schists, where infiltrated H_2O-rich fluid promoted decarbonatization reactions in carbonates. Consequently, in the geological environment where clinohumite occurs in marble as the only mineral phase incorporating F and in the vicinity of magmatic intrusion, it is reasonable to assume a subsequent introduction of external Ti-rich fluorinated fluids being responsible for the clinohumite formation. The examples are granulite facies marbles from the In Ouzzal terrane in Algeria (BOUREGHDA et al., 2023) and dolomitic marbles from the Makrohar granulite Belt, in India (KARMAKAR, 2021). Alternatively, internal fluid buffering is preferred to be responsible for clinohumite formation in the marbles enriched in other hydrous silicates which incorporate fluorine and in the geological environment missing syn-metamorphic magmatic activity, as has been invoked for the high-grade marbles of Ambasamudram, in India (SATISH-KUMAR & NIIMI, 1998; SATISH-KUMAR, 1999).

The origin of the titanium- and fluorine-rich fluid necessary for the Ti-clinohumite formation at the expense of the forsterite in grey marbles of Mt. Moslavačka Gora is not easy to determine, because these marbles contain pargasite and phlogopite, so the possibility for internal fluid buffering exists. As described previously, marbles occur as interlayers within amphibolite and diopside-amphibole schists, which together, represent the fragments of older metamorphic rocks incorporated into granitoid intrusion (Fig. 2). Additionally, in the Kamenac Creek, which is situated in the immediate vicinity of Zorovac Creek, PAMIĆ (1987), described the abandoned quarry of granite, monzodiorite and gabbro. We also found, although not at the primary outcrop, fragments of light-coloured magmatic rock, only 30 m away from the marbles. This rock was not previously described in the literature. It is a piece of alkali feldspar syenite, composed mainly of microcline, orthoclase, diopside, slightly altered to actinolite, and titanite (Fig. 21). Direct contact of the marbles or amphibolite and diopside-amphibole schists fragments with any of these magmatic bodies was not observed, since a large part of the outcrop is covered by vegetation and soil. However, all these magmatic rocks, as well as the metamorphic ones, when linked to magmatic heat input, could be the source of the titanium- and fluorine-rich fluids, responsible for the clinohumite formation.

It is important to emphasize that in the grey marbles of Mt. Moslavačka Gora, no textural evidence supports the reaction between Ti-clinohumite and pargasite and phlogopite, except for one phlogopite flake which looks to be more of a late mineral phase than a product of a restitic primary phase (Fig. 11). Additionally, the extremely rare occurrence of ilmenite, solely as tiny inclusions in spinel and pargasite, could not be taken as a sufficient source of titanium in isochemical reactions of the Ti-clinohumite formation. Recently GARAŠIĆ et al. (2024), reported on Ti-rich hydrothermal fluids causing the replacement of Ti-poor dumortierite, by secondary Ti-rich dumortierite in a pegmatite dyke cutting through Cretaceous leucogranite, in the magmatic-metamorphic complex of Mt. Moslavačka Gora. Therefore, it seems reasonable to conclude that internal fluid buffering may not have been involved, or at least not contributed significantly, to the Ti-clinohumite formation in Mt. Moslavačka Gora, and to prefer an infiltration of Ti- and F-rich hydrothermal fluids from magmatic or metamorphic rocks linked to the magmatic heat input.

Further investigations of these marbles should include stable carbon and oxygen isotopes as well as REE analyses. Both have been shown to be useful in attempting to trace the fluid infiltration in granulite facies marbles as reported for instance by BOULVAIS et al. (2000) and GALLIEN et al. (2009).

5.4. Petrogenesis

It can be deduced from the mineral composition and chemistry as well as the microstructural mineral relationships, that the studied grey marbles experienced at least three different evolutionary stages leading to the formation of specific mineral assemblages: a) the regional metamorphic stage characterised by a peak metamorphic stage in granulite facies and the formation of mineral assemblage consisting of calcite + dolomite + forsterite + spinel + pargasite + phlogopite + ilmenite + apatite, b) the stage of subsequent infiltration of an external Ti-rich, fluorinated fluid from the surrounding magmatic rocks (granite, monzodiorite, gabbro, alkali feldspar syenite) or from an associated metamorphic one (amphibolite, diopside-amphibole schists), linked to magmatic heat input, giving rise to the origin of Ti-clinohumite, c) the stage of uplift and exhumation causing diverse retrograde metamorphic reactions such as the replacement of clinohumite, spinel and pargasite by chlorite, formation of tremolite on the rims of pargasite and forsterite, as well as the replacement of forsterite by serpentine and talc.

5.4.1. The regional metamorphic stage

The marble occurrence as interlayers up to 50 cm thick in amphibolite and diopside-amphibole schists on the bank of the Zorovac Creek may be explained by the existence of one volcano-sedimentary basin within which the sporadic deposition of silicate detritus characterised carbonate sedimentation. This led to the formation of impure dolomite limestone – marble protolith. Silicate-rich tiny bands (Fig. 4) probably reflect a primary bedding. In the framework of the regional metamorphic stage, the marble protolith underwent prograde metamorphism that produced a mineral assemblage consisting of calcite + dolomite + forsterite + spinel + pargasite + phlogopite + ilmenite + apatite. This mineral assemblage is described as a typical high-grade assemblage in many granulite facies marbles worldwide, for instance in impure dolomitic marbles from East Greenland (BUCHER-NURMINEN, 1982), in aluminous calcite-dolomite marbles from the Greek Rhodope massif (PROYER et al., 2008), in metacarbonate rocks from the Mogok metamorphic belt in Myanmar (YE KYAW THU & ENAMI, 2018) et cetera. In contrast to our study, CRNKO & VRAGOVIĆ (1990) associated the marbles of Mt. Moslavačka Gora with hornblende and pyroxene hornfels facies. Although there is no microstructural evidence for the way forsterite, spinel, pargasite and phlogopite formed in the studied grey marbles, it is most probable that during

prograde reactions, dolomite reacted with quartz and H_2O to form calcite and tremolite, which further reacted with the dolomite leading to forsterite and calcite formation. Possible precursors for the spinel formations are corundum, chlorite, anorthite and garnet (PROYER et al., 2008). The origin of phlogopite in the marble may be explained by decarbonatisation reaction in which dolomite, K-feldspar and H_2O react to produce phlogopite, calcite and CO_2 (SATISH-KUMAR et al., 2001). A likely reaction responsible for the pargasite formation includes the reaction between plagioclase, dolomite, quartz and H_2O which may lead to the development of pargasite, calcite and CO_2 (SATISH-KUMAR et al., 2001). Rare ilmenite and apatite are most likely the oldest preserved mineral phases.

It is important to note that in the amphibolites of Mt. Moslavačka Gora, two metamorphic events were recognized. The first one is characterised by a temperature range from 550 ºC to 820 ºC and pressures varying between 520 and 960 MPa (unknown age), whereas the younger one represents low pressure / high temperature metamorphism recording temperatures between 550 ºC and 650 ºC and pressure from 180 to 250 (400) MPa (BALEN et al., 2000). Recent investigation of amphibolite xenoliths in Cretaceous granite (PETRINEC et al., 2022) provided even narrower conditions of amphibolite formation (630 – 700 °C, 800 – 950 MPa) corresponding to upper amphibolite to granulite facies conditions. Ar-Ar amphibole dating in the amphibolites gave an Early Late Cretaceous age (80 – 90) Ma, as reported by BALEN et al. (2001). Similar values (90 – 100 Ma) were documented by monazite dating in metapelites and interpretated as a granulite facies LP/HT metamorphic overprint at 750 ºC and 3 – 4 kbar (STARIJAŠ et al., 2010). Radiometric dating of magmatic zircon cores in orthogneisses provided an Ordovician formation age (≈ 486 ± 6 Ma) which led STARIJAŠ et al. (2010) to conclude that the metamorphic complex of the Mt. Moslavačka Gora predominantly represents a remnant of Ordovician granitic rock associated with the northern Gondwana margin. No radiometric ages were determined in the marbles.

Considering the mineral assemblages and mineral chemistry determined in the marbles, the observed earlier granulite-facies metamorphism, could correspond to the first metamorphism determined by BALEN et al. (2000) in the amphibolites (temperature range from 550 ºC to 820 °C and pressure between 520 and 960 MPa), and amphibole-bearing xenoliths in granite reaching ≈ 8 kbar and max. ≈ 800 °C (PETRINEC & BALEN, 2014) or an even older one, but certainly not to the second one being characterized by a LP/HT metamorphic overprint.

5.4.2. Stage of the subsequent infiltration of an external Ti-rich, fluorinated fluid

The fact that neither the replacement of fluorine-rich minerals such as pargasite and phlogopite nor replacement of titanium-rich ilmenite with Ti-clinohumite have been observed in the samples (Figs. 8, 10), indicates that it was most likely the subsequent infiltration of an external Ti-rich, fluorinated fluid into the marble that was involved in the origin of Ti-clinohumite. Such infiltration may be associated with Ti- and F-rich hydrothermal fluids from the surrounding magmatic rocks such as granite (Fig. 2) the radiometric age of which corresponds to 82 ± 1 Ma according to STARIJAŠ et al. (2010), or monzodiorite and gabbro (PAMIĆ, 1987), or alkali feldspar syenite (this work). However, infiltration may also be explained by the dehydration processes of biotite and/or amphibole from the associated metamorphic rocks (amphibolite, diopside-amphibole schists, metapelite) linked to magmatic heat input. Partial melting reactions in the metapelitic rocks of Mt. Moslavačka Gora was described by PETRINEC & BALEN (2014, 2019) and in the amphibolite xenoliths (PETRINEC et al., 2022). Such processes in Mt. Moslavačka Gora according to the aforementioned authors preceded the granite intrusion. The occurrence of cracks and microfaults in marbles which can be caused by the emplacement of a magmatic body, as also increased porosity caused by decarbonation reactions, in marbles may smooth the way for fluid infiltration. Future stable carbon and oxygen isotope, as well as REE analyses, could provide additional evidence for supporting the idea of external fluid infiltration.

5.4.3. The stage of uplift and exhumation

An incomplete reequilibration of the mineral assemblages to lower temperatures and pressures during uplift and exhumation of the granulite-facies marble of Mt. Moslavačka Gora resulted in the development of diverse retrograde reactions, including the replacement of clinohumite, spinel and pargasite by chlorite (Fig. 11a, b; reaction 2), formation of tremolite on the rims of pargasite and forsterite (Figs. 7, 8; reaction 4), as well as the replacement of forsterite by serpentine and talc (Figs. 5b; reactions 5, 6). The narrow extent of retrograde reactions such as those involved in the occurrence of talc and serpentine suggest that small amounts of H_2O and CO_2 rich fluids were accessible during marble uplift. The processes of uplift and exhumation are most probably linked to the Miocene vertical faulting when according to KOROLIJA et al. (1986) the crystalline complex of Mt. Moslavačka Gora became a horst.

5.5. Clinohumite-bearing marbles from the regional context

The mineral assemblage consisting of Ti-clinohumite + forsterite + spinel + calcite was described in banded marbles occurring along the eastern margin of the Tertiary Bergell contact aureole (the border between Switzerland and Italy) by GIERE (1987). He did not analyse the geological evolution of the area. PROYER et al. (2008) reported on the marbles associated with 170 – 160 Ma old metabasic and metapelitic country rocks, as well as diamond-bearing garnet gneisses in the Kimi complex of the Greek Rhodope metamorphic province. They found different parageneses of calcite, dolomite, diopside, forsterite, spinel, pargasite, Ti-clinohumite and phlogopite in marbles and concluded that silicate and oxide phases of the marbles do not contain evidence of an ultrahigh-pressure metamorphism. FRANZ & ACKERMAND (1980) studied the mineral assemblages consisting of calcite, dolomite, tremolite, diopside, forsterite, clinohumite-titanian clinohumite, chondrodite, chlorite-serpentine, brucite, karlite and ludwigite in marbles from the Schlegeistal in the Western Tauern Area, of the Tyrol in Austria. These marble occurrences

are similar to those in Mt. Moslavačka Gora, forming layers within amphibolites adjacent to metatonalites. They recognised three events in the geological evolution of this area: firstly, a metamorphism of Variscan or pre-Variscan age, a second one associated with the Variscan tonalite intrusion accompanied by a metasomatism and possible clinohumite formation and the last one corresponding to alpine metamorphism including the breakdown of clinohumite, forsterite and diopside. Ti-clinohumite bearing marble lenses also occur within the polymetamorphic Ötztal crystalline complex in the Eastern Alps in Austria, where evidence for pre-Variscan, Variscan and Eo-Alpine metamorphic history were found (THONY et al., 2008). Three different stages in the metamorphic evolution of dolomite marbles in Strážek and Moravian Moldanubicum in the Czech Republic were described by NOVAK & HOUZAR (1996). Dolomite marbles occur as either lenticular bodies in migmatized biotite gneiss or associated with amphibolites at the rim of the Trebič Durbachite Massif. Based on different mineral assemblages consisting of tremolite, phlogopite, dolomite, calcite, forsterite, chlorite, spinel and clinohumite, these authors recognized older HT/HP–MP metamorphism, HT/LP metamorphism associated with the intrusion of the Třebič Durbachite Massif (343 Ma) and retrograde MT–LT/LP metamorphism.

Although three different stages of geological evolution are usually documented in many of the clinohumite-bearing marbles in adjacent regional geological units, they cannot be easily correlated with those observed in the Ti-clinohumite-bearing marbles of Mt. Moslavačka Gora. Namely, there are differences in the age determination of both, metamorphic stages and magmatic intrusions, at least at this stage of the investigation.

6. CONCLUSION

The following conclusions have been drawn from the first systematic investigation of the mineral relationships and reactions, as well as the mineral chemistry in the marbles from Zorovac Creek in Mt. Moslavačka Gora:

The protolith of the studied marbles most likely originated by sporadic deposition of silicate detritus during carbonate sedimentation in a volcano-sedimentary basin.

The first metamorphism had a regional character leading to marble formation with a peak metamorphic stage in the granulite facies and a mineral assemblage consisting of calcite + dolomite + forsterite + spinel + pargasite + phlogopite + ilmenite + apatite. It could correspond to: a) the first metamorphism determined in amphibolites by BALEN et al. (2000) with a temperature range from 550 °C to 820 °C and pressure between 520 and 960 MPa), b) metamorphism observed in amphibole-bearing xenoliths in granite reaching ≈ 8 kbar and max. ≈ 800 °C (PETRINEC & BALEN, 2014), c) an even older metamorphism.

The increase of temperature and/or decrease of X_{CO2} in the system by infiltration of hydrated, fluorinated Ti-rich fluids gave rise to the formation of clinohumite during the second stage. Such infiltration may be associated with Ti- and F-rich hydrothermal fluids from intruded magmatic rocks or with dehydration processes from metamorphic rocks linked to magmatic heat input.

Subsequent uplift and exhumation of the terrain resulted in diverse retrograde metamorphic reactions such as the replacement of clinohumite, spinel and pargasite by chlorite, the formation of tremolite on the rims of pargasite and forsterite, as well as the replacement of forsterite by serpentine and talc.

ACKNOWLEDGEMENT

This work was supported financially by a grant from the University of Zagreb, number 113400112/2023, leader prof. dr. Dunja ALJINOVIĆ. Prof. Dr. Rainer ALTHERR, University of Heidelberg, Faculty of Chemistry and Geosciences, Institute of Earth Sciences, provided access to the microprobe at the Institute for petrography and geochemistry of the Fridericiana University of Karlsruhe, Germany. His continued support and helpful advice in work with the microprobe are gratefully acknowledged. We are sincerely grateful to the anonymous reviewers for the valuable comments which helped to improve our manuscript.

REFERENCES

ANOVITZ, L.M. & ESSENE, E.J. (1987): Phase equilibria in the system $CaCO_3$-$MgCO_3$-$FeCO_3$.– Journal of Petrology, 28, 389–414. https://doi.org/10.1093/petrology/28.2.389

BALEN, D. (2007): Tourmaline nodules occurrence in Moslavačka Gora (Croatia) granite: a snapshot of magmatic processes:– In: 8th Workshop on Alpine Geological Studies. University of Bonn, Bonn, 3–3.

BALEN, D. & BROSKA, I. (2011): Tourmaline nodules – products of devolatilization within the final evolutionary stage of granitic melt?– In: SIAL, A.N., BETTANCOURT, J.S., DE CAMPOS, C.P. & FERREIRA, V.O. (eds): Granite-Related Ore Deposits.– Special Publication of the Geological Society of London, 350, 53–68. https://doi.org/10.1144/SP350.4

BALEN, D. & PETRINEC, Z. (2010): Complex Cretaceous evolution of the Moslavačka Gora crystalline: different aspects from various types of „foreign" and „cognate" enclaves inside granites.– In: HORVAT, M. (ed): 4th Croatian Geological Congress: Abstracts Book. Zagreb, 135–136.

BALEN, D. & PETRINEC, Z. (2011): Contrasting tourmaline types from peraluminous granites: a case study from Moslavačka Gora (Croatia).– Mineralogy and Petrology, 102, 117–134. https://doi.org/10.1007/s00710-011-0164-8

BALEN, D., BELAK, M., TIBLJAŠ, D. & TOMAŠIĆ, N. (2000): The succession of metamorphic paragneisses in mineral assemblage from marble Zorovac Creek (Moslavačka gora, Northern Croatia).– In: Second Croatian Geological Congress: Proceedings. Zagreb, Croatian Geological Survey, 93–96.

BALEN, D., SCHUSTER, R. & GARAŠIĆ, V. (2001): A new contribution to the geochronology of Mt. Moslavačka Gora (Croatia).– In: ÁDAM, A., SZARKA, L. & SZENDRőI, J. (eds): PANDCARDI.– Geodetic and geophysical Research Institute, Šopron, 2–3.

BALEN, D., SCHUSTER, R., GARAŠIĆ, V. & MAJER, V. (2003): The Kamenjača olivine gabbro from Moslavačka gora (South Tisia, Croatia).– Rad Hrvatske akademije znanosti i umjetnosti, 486, 27, 57–76.

BARIĆ, LJ. (1972): Kontaktnometamorfni mramori iz okolice Podgarića u Moslavačkoj gori (Hrvatska) [*Contact metamorphic marbles from the surrounding area of Podgarić in Mt. Moslavačka Gora (Croatia) – in Croatian*].– In: VII kongres geologa SFRJ: Predavanja, knjiga 2, Zagreb. 1–28.

BOULVAIS, P., FOURCADE, S., MOINE, B., GRUAU, G. & CUNEY, M. (2000): Rare earth elements distribution in granulite-facies marbles: a witness of fluid-rock interaction.– Lithos 53, 117–126. https://doi.org/10.1016/S0024-4937(00)00013-X

BOUREGHDA, N., OUZEGANE, K., AÏT-DJAFER, S., BENDAOUD, A., ZOHEIR, B.A. & KIENAST, J.-R. (2023): Ba-rich phlogopite, dissakisite-(Ce), and fluorine-rich clinohumite in granulite-facies marbles from the in Ouzzal terrane, Western Hoggar, Algeria.– Mineralogy and Petrology, 117, 99–111. https://doi.org/10.1007/s00710-022-00802-1

BUCHER-NURMINEN, K. (1982): Mechanism of mineral reactions inferred from textures of impure dolomitic marbles from East Greenland.– Journal of Petrology, 23/3, 325–343. https://doi.org/10.1093/petrology/23.3.325

CHEN, Y., ZHANG, L., ZHANG, G. & LÜ, Z. (2022): The calcite-dolomite solvus temperature and T-X (CO_2) evolution in high-grade impure marble from Thongmön area, Central Himalaya: implications for carbon cycling in orogenic belts.– Minerals, 12, 724. https://doi.org/10.3390/min12060724

COHEN, E. (1887): Andalusitführende granite.– Neues Jahrbuch für Mineralogie, Geologie und Paläontologie, 2, 178–180.

CRNKO, J. (1990): Osnovna geološka karta Republike Hrvatske 1:100 000, list Kutina L 33-90 [*Basic Geological Map of the Republic of Croatia 1:100.000, Kutina sheet L 33-94* – in Croatian].– Hrvatski geološki institut, Zagreb, 2014.

CRNKO, J. & VRAGOVIĆ, M. (1990): Osnovna geološka karta Republike Hrvatske 1:100 000. Tumač za list Kutina L 33-94 [*Basic Geological Map of the Republic of Croatia 1:100 000, Explanatory notes for the Kutina sheet L 33-94* – in Croatian].– Hrvatski geološki institute, Zagreb, 2014.

EVANS, B.V. & TROMMSDORFF, V. (1983): Fluorine hydroxyl titanian clinohumite in Alpine recrystallized garnet peridotite: compositional controls and petrologic significance.– American Journal of Sciences, 283A, 355–369.

FERNANDES, M.L.S. & CHAVES, A.O. (2014): Chemical composition and genesis of the clinohumites from marbles of Itaoca-Gironda, Espirito Santo State, Brazil.– Comunicações Geológicas, 101, Especial I, 81–84.

FRANZ, G. & ACKERMAND, D. (1980): Phase relations and metamorphic history of a clinohumite-chlorite-serpentine-marble from the Western Tauern Area (Austria).– Contribution to Mineralogy and Petrology, 75, 97–110. https://doi.org/10.1007/BF00389771

GALLIEN, F., MOGESSIE, A., BJERG, E., DELPINO, S. & CASTRO DE MACHUCA, B. (2009): Contrasting fluid evolution of granulite-facies marbles: implications for a high-T intermediate-P terrain in the Famatinian Range, San-Juan, Argentina.– Mineralogy and Petrology, 95, 135–157. https://doi.org/10.1007/s00710-008-0026-1

GARAŠIĆ, V. (1993): Metamorfni uvjeti stijena amfibolitnog facijesa Moslavačke gore. [*Metamorphic conditions of rocks of amphibolite facies of Mt. Moslavačka Gora* – in Croatian].– Unpubl. Magister Thesis, Faculty of Science, University of Zagreb, 171 p.

GARAŠIĆ, V., KRŠINIĆ, A., SCHUSTER, R. & VRKLJAN, M. (2007): Leucogranite from Srednja Rijeka (Moslavačka Gora, Croatia).– In: 8th Workshop on Alpine Geological Studies, University of Bonn, Bonn, 21–21.

GARAŠIĆ, V., LUGOVIĆ, B., SEKUŠAK, M., BILIĆ, Š., MEYER, H.-P., SCHUSTER, R. & VRKLJAN, M. (2024): First occurrence of dumortierite in Croatia: its chemical composition and appearance as an igneous mineral in leucogranite-hosted pegmatite.– Geologia Croatica, 77/1, 41–56. https://doi.org/10.4154/gc.2024.01

GASPAR, J.C. (1992): Titanian clinohumite in the carbonatites of the Jacupiranga Complex, Brazil: Mineral chemistry and comparison with titanian clinohumite from other environments.– American Mineralogist, 77, 168–178.

GIERÉ, R. (1987): Titanian clinohumite and geikielite in marbles from the Bergell contact aureole.– Contribution to Mineralogy and Petrology, 96, 496–502. https://doi.org/10.1007/BF01166694

GIL IBARGUCHI, J.I., ABALOS, B., AZCARRAGA, J. & PUELLES, P. (1999): Deformation, high-pressure metamorphism and exhumation of ultramafic rocks in a deep subduction/collision setting (Cabo Ortegal, NW Spain).– Journal of Metamorphic Geology, 17, 747–764. https://doi.org/10.1046/j.1525-1314.1999.00227.x

GOLDSHMIDT, J.R. & NEWTON, R.C. (1969): P-T-X relations in the system $CaCO_3$-$MgCO_3$ at high temperatures and pressures.– American Journal of Science, 267-A, 160–190. https://doi.org/10.2475/001c.125217

HEY, M.H. (1954): A new revies of the chlorites.– Mineral Magazine, 224, 277–292. https://doi.org/10.1180/minmag.1954.030.224.01

HIROI, Y. & KOJIMA, H. (1988): Petrology of dolomitic marbles from the Kasumi rock Prince Olav Coast East Antarctica.– In: Proceedings of the National Institute of Polar Research Symposium on Antarctic Geosciences, 2, National Institute of Polar Research, 96–109.

HUGHES, L. & PAWLEY, A. (2019): Fluorine partitioning between humite-group minerals and aqueous fluids: implications for volatile storage in the upper mantle.– Contributions to Mineralogy and Petrology, 174, 78. https://doi.org/10.1007/s00410-019-1614-2

JONES, N.W., RIBBE, P.H. & GIBBS, G.V. (1969): Crystal chemistry of humite minerals.– American Mineralogist, 54, 391–411.

KARMAKAR, S. (2021): Formation of clinohumite ± spinel in dolomitic marbles from the Makrohar Granulite Belt, Central India: Evidence for Ti mobility during regional metamorphism.– American Mineralogist, 106, 1818–1827.

KIŠPATIĆ, M. (1887): Olivinski gabro iz Moslavačke gore (hiperstenit) [*Olivine gabbro from the Mt. Moslavačka Gora (hyperstenite)* – in Croatian].– Rad JAZU, 95, 24–51.

KOROLIJA, B. & CRNKO, J. (1985): Osnovna geološka karta SFRJ 1:100 000, list Bjelovar, L 33-82 [*Basic Geological Map of SFRY 1 100 000, Bjelovar sheet L 33-82* – in Croatian].– Institut za geološka istraživanja, Zagreb, Savezni geološki zavod, Beograd.

KOROLIJA, B., VRAGOVIĆ, M., CRNKO, J. & MAMUŽIĆ, P. (1986): Osnovna geološka karta 1: 100 000. Tumač za list Bjelovar L 33-82 [*Basic Geological Map of SFRY 1:100 000. Explanatory notes for the Bjelovar sheet L 33-82* – in Croatian].– Institut za geološka istraživanja, Zagreb, Savezni geološki zavod, Beograd.

LEAKE, B.E., WOLLEY, A.R, ARPS, C.E.S., BIRCH, W.D, GILBERT, M.C., GRICE, J.D., HAWTHORNE, F.C., KATO, A., KISCH, H.J., KRIVOVICHEV, V.G., LINTHOUT, K., LAIRD J.O., MANDARINO, J.A., MARESH, W.V., NICKEL, E.H., ROCK, N.M.S., SCHUMACHER, J.C., SMITH, D.C., STEPHENSON, N.C.N., UNGARETTI, L., WHITTAKER, E.J.W. & YOUZHI, G. (1997): Nomenclature of amphiboles; report of the subcommitte on amphibole of the International Mineralogical Association, Commission on New Minerals and Mineral.– The Canadian Mineralogist, 35, 219–246.

LETARGO, C.M.R., LAMB, W.M. & PARK, J.S. (1985): Comparison of calcite + dolomite thermometry and carbonate + silicate equilibria: constraints on the conditions of metamorphism of the Llano uplift, central Texas, U.S.A.– American Mineralogist, 80, 131–143. https://doi.org/10.2138/am-1995-1-213

MCGETCHIN, T.R., SILVER, L.T. & CHODOS, A.A. (1970): Titanoclinohumite: a possible mineralogical site for water in the upper mantle.– Journal of Geophysical Research, 75, 2, 255–259. https://doi.org/10.1029/JB075i002p00255

MENZEL, M.D., GARRIDO, C.J., SÁNCHEZ-VIZCAINO, V.L., HIDAS, K. & MARCHESI, C. (2019): Subduction metamorphism of serpentinite-hosted carbonates beyond antigorite-serpentinite dehydration (Nevado-Filábride Complex, Spain).– Journal of Metamorphic Geology, 37, 681–715. https://doi.org/10.1111/jmg.12481

MIZUOCHI, H., SATISH-KUMAR, M., MOTOYOSHI, Y & MICHIBAYASHI, K. (2010): Exsolution of dolomite and application of calcite-dolomite solvus geothermometry in high-grade marbles: an example from Skallevikshalsen, East Antarctica.– Journal of metamorphic Geology, 28, 509–526. https://doi.org/10.1111/J.1525-1314.2010.00877.X

NISHIO, I., MORISHITA, T., SZILAS, K., PEARSON, G., TANI, K.-I., TAMURA, A., HARIGANE, Y. & GUOTANA, J.M. (2019): Titanian clinohumite-bearing peridotite from the Ulamertoq ultramafic body in the 3.0 Ga Akia Terrane of Southern West Greenland.– Geosciences, 9/153, 1–20. https://doi.org/10.3390/geosciences9040153

NOVAK, M. & HOUZAR, S. (1996): The HT/LP metamorphism of dolomite marbles in the eastern part of the Moldanubicum; a manifestation of heat

flow related to the Třebič Durbachite Massif.– Journal of the Czech Geological Society, 41/3–4, 139–146.

PALINKAŠ, A.L., BALOGH, K., STRMIĆ, S., PAMIĆ, J. & BERMANEC, V. (2000): Ar/Ar dating and fluid inlusion study of muscovite, from the pegmatite of Srednja Rijeka, within granitoids of Moslavačka gora Mt., North Croatia.– In: TOMLJENOVIĆ, B., BALEN, D. & SAFTIĆ, B. (eds): PANCARDI 2000.– Special Issue, Vijesti Hrvatskog geološkog društva, 37, 95–96.

PAMIĆ, J. (1987): Granites and associated monzodiorites and gabbros from Kamenac Creek on Mt. Moslavačka Gora (Northern Croatia, Yugoslavia).– Rad JAZU, 431/22, 179–199.

PAMIĆ, J. (1990): Alpine granites, migmatites and metamorphic rocks from Mt. Moslavačka Gora and the surrounding basement of the Pannonian Basin (Northern Croatia, Yugoslavia).– Rad JAZU, 10, 7–121.

PAMIĆ, J. (1998): Crystalline basement of the South Pannonian Basin based on surface and subsurface data.– Nafta, 49, 371–390.

PAMIĆ, J. & JURKOVIĆ, I. (2002): Palaeozoic tectonostratigraphic units of the northwest and central Dinarides and the adjoining South Tisia.– International Journal of Earth Sciences, 91, 787–798. https://doi.org/10.1007/s00531-001-0229-8

PETRINEC, Z. & BALEN, D. (2014): Cretaceous evolution of the Adria-Europe plate boundary: succession of events recorded in granites and enclaves of the Moslavačka Gora (Croatia).– In: EGU General Assembly 2014, Abstracts & Programme, EGU2014-6186-x.

PETRINEC, Z. & BALEN, D. (2019): Cordierite-producing reactions in anatectic rocks from Moslavačka Gora (Croatia).– In: HORVAT, M., MATOŠ, B. & WACHA, L. (eds.): 6th Croatian Geological Congress: Abstracts Book.– Croatian Geological Survey, Zagreb, 156–157.

PETRINEC, Z., BALEN, D., LADIŠIĆ, A. & OLIĆ, I. (2022): Mesozoic subduction-related metamorphic record from amphibolites of Sava zone: Moslavačka Gora (Croatia).– In: Goldschmidt: Abstract Book, Honolulu. https://doi.org/10.46427/gold2022.10484

PIAZOLO, S. & MARKL, G. (1999): Humite- and scapolite-bearing assemblages in marbles and calcsilicates of Dronning Maud Land, Antarctica: new data for Gondwana reconstructions.– Journal of metamorphic Geology, 17, 91–107. https://doi.org/10.1046/j.1525-1314.1999.00179.x

POWELL, R., CONDELIFFE, D.M. & CONDELIFFE, E. (1984): Calcite-dolomite geothermometry in the system $CaCO_3$-$MgCO_3$-$FeCO_3$: an experimental study.– Journal of Metamorphic Geology, 2, 3341. https://doi.org/10.1111/j.1525-1314.1984.tb00283.x

PRADEEPKUMAR, A.P. & KRISHNANATH, R. (1996): Rare earth element mobility in halogenated aqueous fluids in the humite-marbles of Ambasamudram, Kerala Khondalite Belt, India.– Current Science, 70, 1066–1074.

PRADEEPKUMAR, A.P. & KRISHNANATH, R. (2000): A Pan-African „Humite epoch" in East Gondwana: implications for Neoproterozoic Gondwana geometry.– Journal of Geodynamics, 29, 43–62. https://doi.org/10.1016/S0264-3707(99)00062-9

PROYER, A., MPOSKOS, E., BAZIOTIS, I. & HOINKES, G. (2008): Tracing high-pressure metamorphism in marbles: Phase relations in high-grade aluminous calcite-dolomite marbles from the Greek Rhodope massif in the system CaO-MgO-Al_2O_3-SiO_2-CO_2 and indications of prior aragonite.– Lithos, 104, 119–130. https://doi.org/10.1016/j.lithos.2007.12.002

RICE, J.M. (1980): Phase Equilibria involving humite mineral sin impure dolomitic limestones: Part I – Calculated stability of clinohumite.– Contribution to Mineralogy and Petrology, 71, 219–235. https://doi.org/10.1007/BF00371664

RIOS, C.A., CASTELLANOS, O.M. & CHACÓN, C.A. (2015): Ti-clinohumite in the Ciénega skarn-type mineralogy, Sierra Nevada de Santa Marta Massif (Colombia): Occurrence and petrologic significance.– Earth Sciences Research Journal, 19,1, 15–30. https://doi.org/10.15446/esrj.v19n1.42020

SÁNCHEZ-VIZCAÍNO, V.L., TROMMSDORFF, V., GÓMEZ-PUGNAIRE, M.T., GARRIDO, C.J., MÜNTENER, O. & CONNOLLY, J.A.D. (2005): Petrology of titanian clinohumite and olivine at the high-pressure breakdown of antigorite serpentinite to chlorite harzburgite (Almirez Massif, S. Spain).– Contribution to Mineralogy and Petrology, 149, 627–646. https://doi.org/10.1007/s00410-005-0678-3

SATISH-KUMAR, M. (1999): An overview of petrology of calc-silicate granulites from the Trivandrum block, Southern India.– Journal of Geosciences, 42, 9, 127–159.

SATISH-KUMAR, M. & NIIMI, N. (1998): Fluorine rich clinohumites from Ambasamudram, southern India: Mineralogic and FTIR spectroscopic characterization.– Mineralogical Magazine, 62, 509–519.

SATISH-KUMAR, M., WADA, H., SANTOSH, M. & YOSHIDA, M. (2001): Fluid-rock history of granulite facies humite-marbles from Ambasamudram, southern India.– Journal of Metamorphic Geology, 19, 395–410. https://doi.org/10.1046/j.0263-4929.2001.00318.x

SCHMID, S.M., BERNOULLI, D., FÜGENSCHUH, B., MATENCO, L., SCHEFER, S., SCHUSTER, R., TISCHLER, M. & USTASZEWSKI, K. (2008): The Alpine-Carpathian-Dinaridic orogenic system: correlation and evolution of tectonic units.– Swiss Journal of Geoscience, 101, 139–183. https://doi.org/10.1007/s00015-008-1247-3

STARIJAŠ, B., GERDES, A., BALEN, D., TIBLJAŠ, D. & FINGER, F. (2010): The Moslavačka Gora crystalline massif in Croatia: A Cretaceous heat dome within remnant Ordovician granitoid crust.– Swiss Journal of Geoscience, 103, 61–82. https://doi.org/10.1007/s00015-010-0007-3

THÖNY, W.F., TROPPER, P., SCHENNACH, F., KRENN, E., FINGER, F., KANIDL, R., BERNHARD, F. & HOINKES, G. (2008): The metamorphic evolution of migmatites from the Ötztal complex (Tyrol, Austria) and constraints on the timing of the pre-Variscan high-T event in the Eastern Alps.– Swiss Journal of Geoscience, 1, 111–126. https://doi.org/10.1007/978-3-7643-9950-4_7

TROMMSDORFF, V. & EVANS, B.V. (1980): Titanian hydroxyl-clinohumite: formation and breakdown in antigorite rocks (Malenco, Italy).– Contribution to Mineralogy Petrology, 72, 229–242. https://doi.org/10.1007/BF00376142

TUĆAN, F. (1904): Pegmatit u kristaliničnom kamenju Moslavačke gore [*Pegmatite in crystalline rocks of Mt. Moslavačka Gora* – in Croatian].– Rad JAZU, 159, 166–208.

TUĆAN, F. (1953): Nov prinos poznavanju kristalastih stijena Moslavačke gore [*New contribution to understanding of crystalline rocks of Mt. Moslavačka Gora* – in Croatian].– In: Spomenica Miše Kišpatića. JAZU, Zagreb, 39–69.

USTASZEWSKI, K., SCHMID, S.M., FÜGENSCHUH, B., TISCHLER, M., KISSLING, E. & SPAKMAN, W. (2008): A map-vies restoration of the Alpine-Carpathian-Dinaridic system for the Early Miocene.– Swiss Journal of Geosciences, 101, 273–294. https://doi.org/10.1007/s00015-008-1288-7

WHITNEY, D.L. & EVANS, B.W. (2010): Abbreviations for names of rock-forming minerals.– American Mineralogist, 95, 185–187.

YE KYAW THU & ENAMI, M. (2018): Evolution of metamorphic fluid recorded in granulite facies metacarbonate rocks from the middle segment of the Mogok metamorphic belt in central Myanmar.– Journal of Metamorphic Geology, 36, 905–931. https://doi.org/10.1111/jmg.12419